Journal of Nanobiotechnology

REVIEW

Open Access

An encounter between metal ions and natural products: natural products-coordinated metal ions for the diagnosis and treatment of tumors

Xinyue Liu[1†], Suyi Liu[2†], Xingyue Jin[2], Haifan Liu[1], Kunhui Sun[2], Xiongqin Wang[3,4], Meifang Li[3,4], Ping Wang[3,4], Yanxu Chang[2], Tiejie Wang[1,3,4*], Bing Wang[3,4*] and Xie-an Yu[3,4*]

Abstract

Natural products-coordinated metal ions to form the nanomedicines are in the spotlight for cancer therapy. Some natural products could be coordinated with metal ions forming nanomedicines via simple and green environmental self-assembly, which not only improved the bioavailability of natural products, but also conferred multiple therapeutic modalities and multimodal imaging. On the one hand, in the weak acidity, glutathione (GSH) and hydrogen peroxide (H_2O_2) overexpression of tumor microenvironment (TME), such carrier-free nanomedicines could be further enhanced the therapeutic effect via optimizing the species of metal ions. On the other hand, nanomedicines could exert the precise treatment of tumor under the guidance of multiple imaging. Hence, this review summarized the research progress in recent years on the application of natural product-coordinated metal ions in cancer therapy. In addition, the prospects and challenges for the application of natural product-coordinated metal ions were discussed, especially how to improve targeting ability and stability and assess the safety of metal ions, so as to facilitate the clinical translation and application of natural product-coordinated metal ions nanomedicines.

Keywords Natural products, Metal ions, Coordination-induced self-assembly, Diagnosis and treatment of tumors, Clinical transformation and application

†Xinyue Liu and Suyi Liu These authors contributed equally.

*Correspondence:
Tiejie Wang
szyjwtj@163.com
Bing Wang
wangbingszyj@163.com
Xie-an Yu
yuxieanalj@126.com
Full list of author information is available at the end of the article

Graphical Abstract

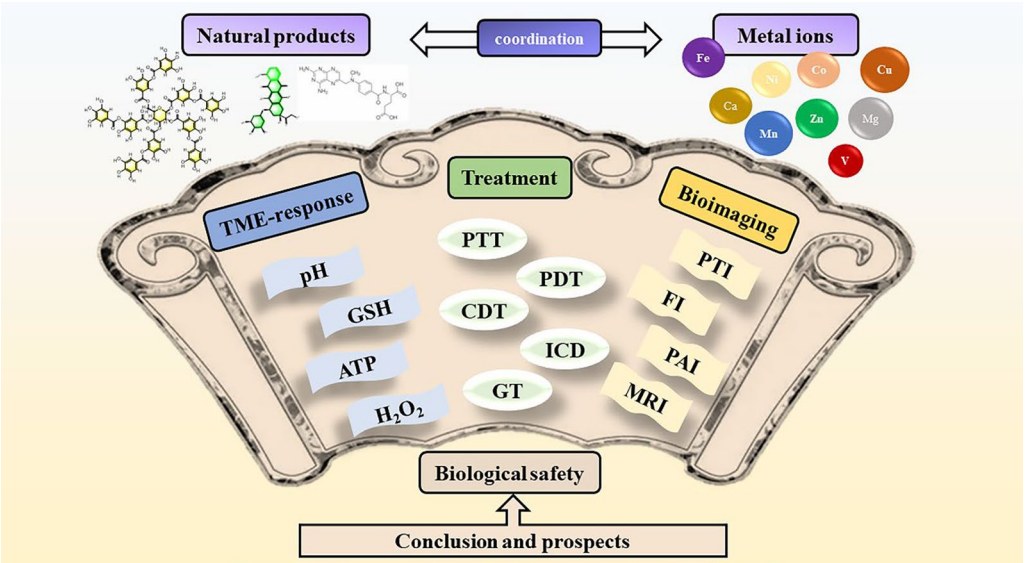

Introduction

Cancer has become a serious challenge to human health and survival. Moreover, complications such as infection, hemorrhage, acidosis, and hypokalemia during tumor development directly affect human health [1, 2]. Traditional therapies such as chemotherapy and radiation present side effects that are impossible to ignore. Such as hematologic toxicity, gastrointestinal reaction, liver toxicity and nervous system toxicity. Therefore, it is urgent to explore effective and safe treatment methods [3]. Recently, nanomedicines formed by natural product-coordinated metal ions have attracted great attention in cancer diagnostics and therapy owing to improve the bioavailability and safety of antitumor drugs, possess multiple therapeutic modalities for precise treatment under imaging monitoring [4–6].

Natural products are chemical components or their metabolites in animals, plants and microorganisms, characterized by abundant sources and novel structures, which are widely recognized for their accessibility, effective activity and safety. Over the years, it has been a valuable and useful source of anticancer agents [7]. Among the various treatments for cancer, traditional Chinese medicine and natural products have an exceptional anticancer effect due to their unique advantages of high efficiency and minor side effects [8]. Currently, natural products have been employed in the green synthesis of nanomaterials to reduce the carbon footprint of the synthesis process. The green synthesis of nanomaterials prepared from natural products is low-cost, less polluting and safe for the environment and human health compared to conventional materials [9]. Notably, prepared green nanomaterials based on natural products also could be applied for the treatment of diseases [10]. Several studies revealed that natural products could remove cancer cells by targeting the tumor immune microenvironment, modulating the cell cycle and promoting apoptosis [11, 12].

Metal ions are essential for the life activities of the vast majority of organisms and, are required to participate in their metabolic processes in order to maintain major physiological functions. It plays an important role in many complex physiological and biochemical processes such as cell division, material transport, metabolic regulation, etc. [13]. With the emergence of the star anti-cancer drug cisplatin, transition metal complexes are also considered to be an effective cancer cell inhibitor [14]. For example, the first-line systemic chemotherapeutic drug doxorubicin (DOX) possesses the characteristics of diagnosis and treatment after coordination with transition metal Fe or Cu. It not only improves the aqueous solubility and bioavailability of DOX, but also enables it to be utilized in multiple treatments and multimodal imaging [15, 16]. Therefore, there are great prospects in the treatment of cancer via the coordination of natural products with metal ions.

Currently, synergistic therapies such as chemodynamic therapy (CDT), photodynamic therapy (PDT) and

photothermal therapy (PTT) based on natural products-coordinated metal ions offer new options for the treatment of tumors [17–19]. Multimodal imaging integrates optical, electrical, magnetic, and nuclide imaging paradigms to achieve cross-scale imaging from the molecular level to the in vivo level and from the angstrom to the meter. Multimodal imaging has been extensively applied in oncology research and other cutting-edge life science fields [20–22]. For example, it could be applied for treatment detection and efficacy assessment of tumors, which was conducive to the realization of precision therapy [23]. In addition, imaging detection was used for tracing of drugs and obtaining the entire drug delivery process. Some imaging detections have been applied in targeting and accumulating primary and metastatic tumors. Therefore, the development of imaging-guided drug delivery as well as the combination of multiple imaging modalities for nanomedicine tracing as well as for tumor diagnosis and therapy is of great significance [24]. After coordinated metal ions, the nanomedicines possess multimodal imaging function includes magnetic resonance imaging (MRI), photothermal imaging (PTI), photoacoustic imaging (PAI), and fluorescence imaging (FI), etc., which enables precise diagnosis and treatment of tumors guided by the combination of multiple imaging modalities. Accordingly, combining the respective advantages of natural products and metal ions, coordination assembly not only features simple and green synthesis and breaks through the limitations of traditional synthesis methods, but also highlights the application of multi-pathway precision therapy guided by multimodal imaging. Obviously, the natural product-coordinated metal ion nanomedicines offer new strategies for tumor therapy.

In this review, we systematically summarized the coordination assembly of natural products with essential metal elements in human body, mainly including therapeutic and biological imaging modalities (Fig. 1). In addition, we provided insights into the potential safety problem, current problems and future prospects of metal coordination. This review provided a scientific basis and outlook for the synthesis of nanomedicines from natural product-coordinated metal ions for the treatment of cancer.

Self-assembly of natural product-coordinated essential metal ions for cancer therapy and diagnosis

With the gradual maturation of nanotechnology, nanomedicines synthesized from natural product-coordinated metal ions are attracting more attention due to their environmentally-friendly synthesis, controllability of size and morphology, stability in body circulation, high drug loading rate and the advantages of multi-pathway, multi-target therapeutics and multi-modal imaging [25]. Current studies have demonstrated the high safety and biocompatibility of supramolecular nanoparticles based on coordination-induced self-assembly. Natural product-coordinated metal ions possessed the performance of responding to the TME for targeted drug release [25, 26]. Self-assembly of natural products with essential metal elements in the human body can not only play the chemotherapeutic effect of natural products, but also improve the microenvironment of the tumor through exogenous supplementation of metal elements to achieve the therapeutic purpose. Essential metal elements include calcium (Ca), magnesium (Mg), iron (Fe), copper (Cu), manganese (Mn), zinc (Zn), cobalt (Co), molybdenum (Mo), nickel (Ni), vanadium (V) and tin (Sn). These elements are essential in the human body and participate in various biochemical reactions, such as energy production, cell division, and immune function, etc. The following section describes the coordination applications of natural products with these metal elements.

Natural product-coordinated Ca^{2+} self-assembly

Calcium, as a macronutrient in the body, is a major component of human bones and teeth. It controls a variety of cellular processes and is essential for maintaining bone health, normal nerve conduction and muscle contraction [27]. Currently, there were few studies on coordination self-assembly nanoparticles of natural products with Ca^{2+}.

In recent years, Yang et al. constructed a composite hydrogel consisting of Au nanocluster and P. aeruginosa microcystis leaf extract by a one-step method along with redox and coordination reactions. They found the synthesized hydrogel demonstrated excellent photothermal performance and significant tumor cell inhibitory activity. In vivo PTI also demonstrated that the hydrogel could be effectively enriched into the tumor site and showed a significant temperature increase under laser irradiation. At the end of the treatment, they noticed that the hydrogel significantly inhibited tumor growth. Importantly, histopathological sections indicated no obvious adverse effects. In conclusion, the hydrogel could coordinate with Ca^{2+} present in the tumor environment, which not only reduced the toxicity and side-effects, but also accumulated in high concentration in the lesion and enhanced the anticancer ability [28]. Representative natural products coordinated with Ca^{2+} were summarized in Table 1.

Natural product-coordinated Mg^{2+} self-assembly

Magnesium is an essential element for sustaining life activities in human body and exerts miraculous functions in regulating nerve, muscle activities and enhancing endurance. Anu et al. developed a cannabidiol–loaded

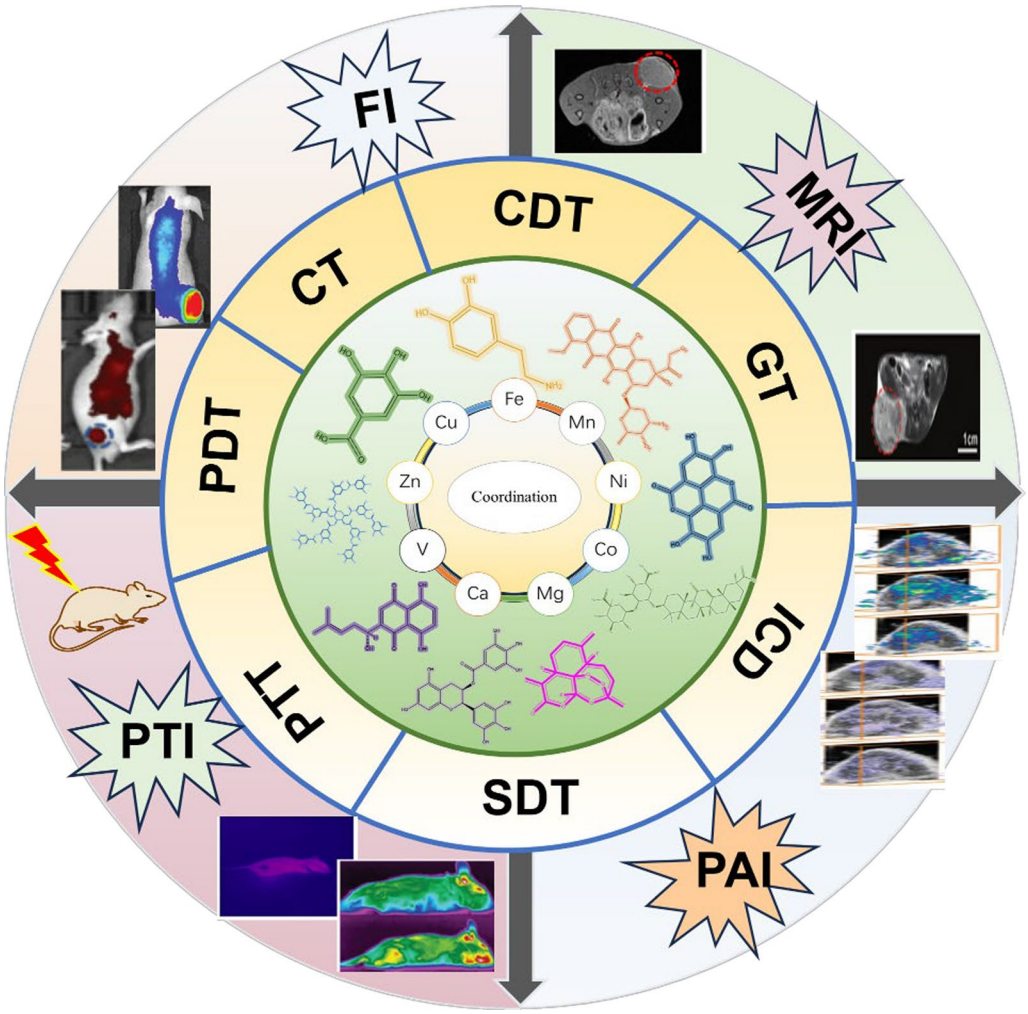

Fig. 1 The therapeutic and biological imaging modalities of metal-coordinated natural product nanoparticles, including multiple therapeutic modalities (CT/ PDT/ PTT/ SDT/ ICD/ GT/ CDT) and multiple biological imaging modalities (MRI/ PAI/ PTI/ FI)

Table 1 Representative natural products coordinated with Ca^{2+} and Mg^{2+}

NO	Natural Products	Metal ions	Preparation	TME Response	Size	Treatment	Bioimaging	Reference
1	Premna microphylla leaf extract, PMLE	Ca^{2+}	*In-vivo* assembly	NIR, pH	–	PTT/PDT	PTI	[28]
2	Gallic acid, GA	Mg^{2+}	Hydrothermal	pH	–	CT/CDT/PTT	–	[29]

Mg–gallate metal–organic framework via Mg^{2+} coordinated with gallic acid (GA) and loaded with cannabidiol (CBD) for the study of anticancer effects in rat glioma brain cancer (C6) cell lines. The fabricated nanomedicines achieved the rapid release of GA and CBD under acidic conditions in vitro confirmed TME response and safety to normal tissues. It could provide two potential anticancer agents (CBD and GA) to the cancer cells at the same time and displayed greater inhibition of C6 glioblastoma cells [29]. Representative natural products coordinated with Mg^{2+} were summarized in Table 1.

Natural product-coordinated $Fe^{2+/3+}$ self-assembly

Iron, the most abundant trace element in the human body, is involved in regulating various physiological functions, such as body metabolism, nutrient synthesis, and regulation of immune function. In recent years, self-assembled structures of natural products coordinated

with $Fe^{2+/3+}$ have been widely investigated and applied in the field of oncology. Currently, extensive researches have confirmed the effect of $Fe^{2+/3+}$ as a catalyst of the Fenton reaction in CDT, which converts H_2O_2 in the endogenous TME into ·OH to kill tumor cells. Furthermore, the introduction of Fe^{3+} depleted high levels of GSH in the tumor environment and enhanced oxidative stress. Therefore, enhanced intracellular CDT in tumor cells by introducing exogenous $Fe^{2+/3+}$ is a promising therapeutic approach. In addition to above potential anticancer applications, iron-containing nanoparticles served as contrast agents for PAI and MRI. Furthermore, $Fe^{2+/3+}$ coordination was demonstrated to possess excellent photothermal properties for applications in PTT and bioimaging.

In recent years, a great number of traditional Chinese medicinal ingredients were also found to possess the ability to coordinate with metals, especially polyphenolic compounds. Tannic acid (TA), a natural product with the ability to coordinate with metal ions, was listed as a food additive by the US Food and Drug Administration [30]. Currently, numerous studies reported that the coordination of TA with Fe^{3+} accelerated the Fenton reaction and enhanced the generation of ·OH, which could serve as a carrier for CDT. In addition, TA-Fe^{3+} complexes presented photothermal properties and imaging functions [31]. Luo et al. prepared DOX-encapsulated nanoparticles by directly attaching Fe^{3+} and TA complexes to DOX. Rupture in the tumor environment released DOX for CT, and the introduction of Fe^{3+} depleted Adenosine triphosphate (ATP) further enhanced the CT effect. The nanoparticles combined with PTT for 14 days resulted in a significant improvement of tumor volume. Moreover, it could be used for MRI, PAI and PTI (Fig. 2a) [32]. Li et al. prepared a nanoplatform for dual-mode MRI-guided combined chemo-photothermal anti-cancer therapy. Fe-TA was adhered to the outer layer of polydopamine (PDA)-modified Fe_2O_3 to form a coordination network magnetic nanoparticles with effective T1/T2 bimodal MRI properties. This nanoparticle not only possessed significant photothermal properties, but also served as an effective delivery platform for the chemotherapeutic drug DOX [33]. The combination of photothermal and immunotherapy provided a great advantage in the treatment of cancer. In another study, TA were attached to the poly (lactic-co-glycolic acid), (PLGA) surface after coordination with Fe^{3+}. The nanoparticles displayed excellent photothermal conversion efficiency and photothermal stability under laser irradiation. The photothermal treatment could induce the release of Damage Associated Molecular Patterns (DAMPs) from effectively triggering the immune response and promoting the maturation of DC cells. The experimental results revealed that the tumor site warmed up significantly after laser irradiation, which effectively inhibited in situ tumor growth. In addition, the distal tumor was also obviously suppressed due to the stimulation of immunogenetics by the laser. The combination of photothermal and immunotherapy provided a new platform for in situ, distal and metastatic tumors [34]. Besides, Tian et al. designed an O_2 self-supplying catalytic nanoparticle for cascade metabolic-CDT based on TA and Fe^{3+} coordination-loaded lactate oxidase via dual depletion of lactate and ATP as well as generation of ·OH [35]. This nano-formulation enables cascade metabolic-CDT. Meanwhile, the TA-coordinated Fe^{3+} appeared photoacoustic signaling that could serve as a guide to improve the accuracy of the therapy.

Zhang et al. designed a nanoparticle consisting of gallic acid (GA) coordinated with Fe^{3+} (Fig. 2b). It possessed satisfactory photothermal stability properties and favorable photothermal conversion efficiency; the nanoparticle prepared was released only under TME. In addition, the nanoparticle could be applied for MRI, which enabled localization of tumor location and volume. The apoptosis-inducing effect of the nanoparticle was also demonstrated at the cellular level. This study enabled CT and PTT synergistic strategy mediated by MRI [36]. On this basis, Liu et al. loaded the DOX into hollow Fe-GA/ bovine serum albumin(BSA), which produced ·OH by depleting intracellular high glutathione (GSH) and triggering the Fenton reaction for CT combined with CDT [37]. Similarly, ellagic acid-coordination Fe^{3+} possessed favorable photothermal properties, and this nanoparticle could massively enrich at the tumor site for MRI and PAI (Fig. 2c) [38].

Dopamine (DA), as a polyphenol compound, had the ability to chelate iron. At the same time, it could be easily polymerized into PDA and widely applied in the nano delivery field. Chen et al. developed a degradable metal complex containing Fe^{3+}-DA (FEP) core and HA-crosslinked Cisplatin (CDDP) shell (PTH), which amplified in situ toxicity of ROS production through synergistic interaction of CDDP and Fe^{3+}. CDDP and Fe^{3+} were continuously released in the TME, which synergistically enhance the effect of CDT and CT through depleting GSH, inhibiting the expression of GPX4, up-regulating expression of p53 and NOXs. In addition, this metal complex exhibited excellent photothermal properties owing to the presence of FEP core, which accelerated the Fenton reaction while playing a role in the PTT effect (Fig. 2d) [39]. Furthermore, Zhang et al. designed the simultaneous application of Fe^{3+} and DA coordination with polyvinylpyrrolidone (PVP) to improve the dispersion stability of the nanoparticles showed good photothermal effects, which allowed for in vitro and in vivo PTI and PAI [40].

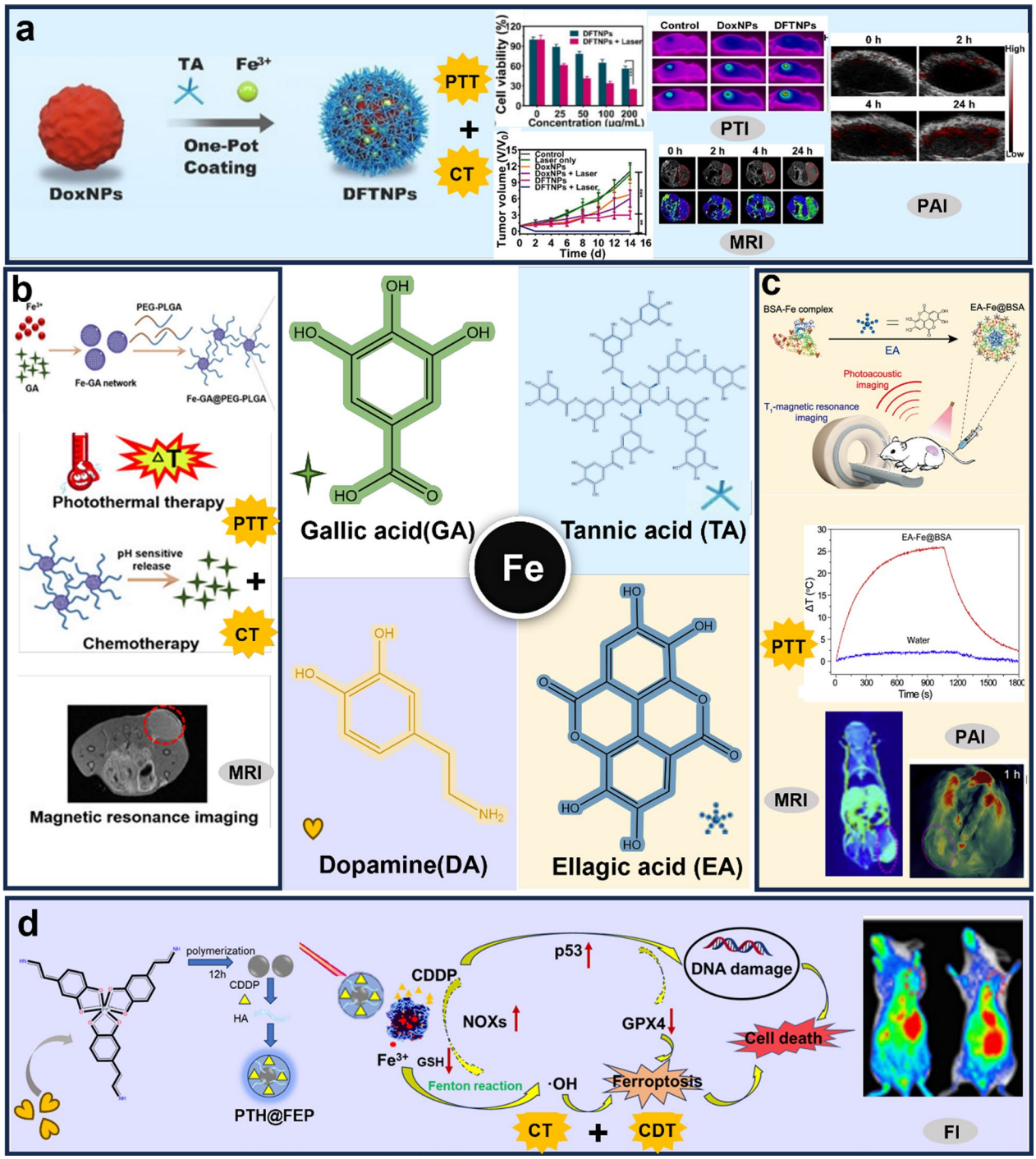

Fig. 2 Some representative natural products coordinated with $Fe^{3+/2+}$. **a** The treatment and bioimaging of tannic acid-coordination Fe^{3+} encapsuled DOX NPs. Copyright 2022, Ivyspring International Publisher. **b** The TME response, treatment and bioimaging of gallic acid-coordination Fe^{3+} and then was encapsuled with PEG-PLGA. Copyright 2022, Dove Medical Press Ltd. **c** The treatment and bioimaging of ellagic acid -coordination Fe^{3+} and then was encapsuled with BSA. Copyright 2022, Dove Medical Press Ltd. **d** The design, mechanism, treatment and bioimaging of PTH@FEP. Copyright 2020, American Chemical Society

Anti-cancer drug coordinated with metal ions conferred multiple therapeutic pathways. Wang et al. synthesized hyaluronic acid (HA)-modified Fe^{3+}-porphyrin (TCPP)-coordinated nanoparticles (FT@HA NPs) using a one-pot method that exhibited FI and MRI properties. The release of Fe^{3+} and TCPP in the low pH and high GSH tumor microenvironment of the tumor triggered GSH depletion and Fenton reaction. At the same time, the fluorescence and PDT effects of TCPP were activated. MRI and FI results revealed the enrichment and metabolism of the nanomedicine at the tumor site, thus enabling the monitoring of the in vivo processes of FT@HA NPs. FT@HA NPs could precisely exert therapeutic effects under the guidance of dual-mode imaging [41]. This nanoplatform integrated PDT, MRI and FI, which highlighted the synergistic therapeutic and imaging effects generated by the coordination of natural products with metal ions. In addition, Xu et al. fabricated a nanoparticle with acid-responsive and ultrasound-enhanced release response, which synthesized from hematoporphyrin monomethyl ether-coordination Fe^{3+}-loaded DOX. The phospholipid modification was more conducive to tumor-targeting enrichment and showed significant tumor inhibitory effects [42]. For systemic delivery and prolonged circulation time, Liang et al. designed a nanoparticle based on DOX-coordination Fe^{3+} and then camouflaged with erythrocyte membranes. It achieved excellent in vitro and in vivo antitumor therapeutic effects [15]. In 2022, Fan et al. designed an anti-angiogenic nanoparticle, which was self-assembled from the chemicals pemetrexed, Fe^{3+} and hyoscine B via coordination-driven self-assembly. The nanoparticle enabled visualized self-targeting under MRI monitoring for effective tumor therapy by inhibiting angiogenesis [43].

In 2021, Chen et al. developed a carrier-free nanoparticle consisting of Fe^{3+} coordinated to artemisinin (ART). Fe^{3+}-ART NPs were employed for MRI and CDT. Interestingly, this was a therapeutic strategy to amplify oxidative stress in vivo, which was independent of H_2O_2 concentration. Fe^{3+} was released with ART in the TME, where Fe^{3+} was reduced to Fe^{2+} by GSH. Then Fe^{2+} catalyzed the breakage of the peroxide bridge bond of ART generating more reactive oxygen species (ROS), thus inducing cell death. In the meanwhile, the depletion of reduced GSH further reduced the antioxidant capacity of tumor cells, exerting a synergistic therapeutic effect. In addition, it was smoothly metabolized in vivo and exerted a favorable biosafety profile due to its biodegradability (Fig. 3a) [44]. Similarly, Li et al. attached TA and Fe^{2+} to ART-coated ZIF skeletons, which caused high levels of ROS and MDA and reduced GSH levels in the cells after treatment. In vitro anti-tumor experiments demonstrated that the nanoparticles had a higher inhibitory activity against tumor cell proliferation compare with monomers [45]. Metal polyphenol networks were also applied in the treatment of gliomas in the brain. Epigallocatechin-3-gallate (EGCG) was first synthesized with HA to form HA-EGCG, and then EGCG was coordinated with Fe^{3+} to prepare a metal-tea polyphenol network targeting delivery of DOX for CDT combined CT of glioma [46].

Numerous studies have demonstrated that shikonin suppressed tumor growth in a variety of ways. Shikonin and Fe^{3+} were formed into spherical homogeneous nanoparticles by coordination-induced self-assembly and wrapped with polyethylene glycol and tumor-targeting moieties to achieve tumor-targeted release (GSH response). Elevated Fe^{2+} levels, GSH depletion, inhibition of GPX4 expression and increased reactive oxygen species induce lipid peroxidation, which led to the onset of ferroptosis. At the same time, the release of shikonin would amplify the degree of intracellular oxidative stress and accelerated tumor cell death through necrotic apoptosis. Additionally, the nanoparticles could be applied to MRI in vivo (Fig. 3b) [47]. This nanoplatform further proved the coordination of natural products and metal ions was an effective strategy for tumor therapy. Similarly, external loading of glucose oxidase and internal loading of the iron apoptosis inducer sorafenib after the coordination of shikonin and Fe^{3+} could lead to ferroptosis [48]. Yu et al. designed a nanoplatform with pH response via green tea polyphenol/iron complex wrapped docetaxel and cynomorium songaricum polysaccharide. The nanoplatform not only showed a favorable PTT effect, but also induced a powerful ICD and promoted an immune response. It was demonstrated that this nanoplatform could inhibit tumor metastasis and recurrence [49].

In another study, GA, 5-fluorouracil and Fe^{3+}, were self-assembled to form GF-Fe NPs based on a polyphenol coordination self-assembly strategy. The GF-Fe NPs encountered cleavage by synthetic desferrioxamine, then GA and 5-fluorouracil were progressively released while the PA signals were attenuated. Real-time accurate quantitative control of drug release in real time guided by PA imaging was achieved by linear fitting between PA signal intensity and the amount of drug release [50]. Modulation of the immune microenvironment to enhance the therapeutic efficacy of tumors yielded fruitful results as well. A well-compatible (pH-responsive) metal-immunopeptide nanocomplex consists of non-covalent interactions between APP (APP is anti-programmed death ligand-1 peptide)-SPM-dextran (DEX) and sodium tripolyphosphate (TPP) as well as coordination between Fe^{3+} and TPP. This complex could generate ROS to induce oxidative stress in tumors, leading to mitochondrial dysfunction, triggering ferroptosis. The protein expression

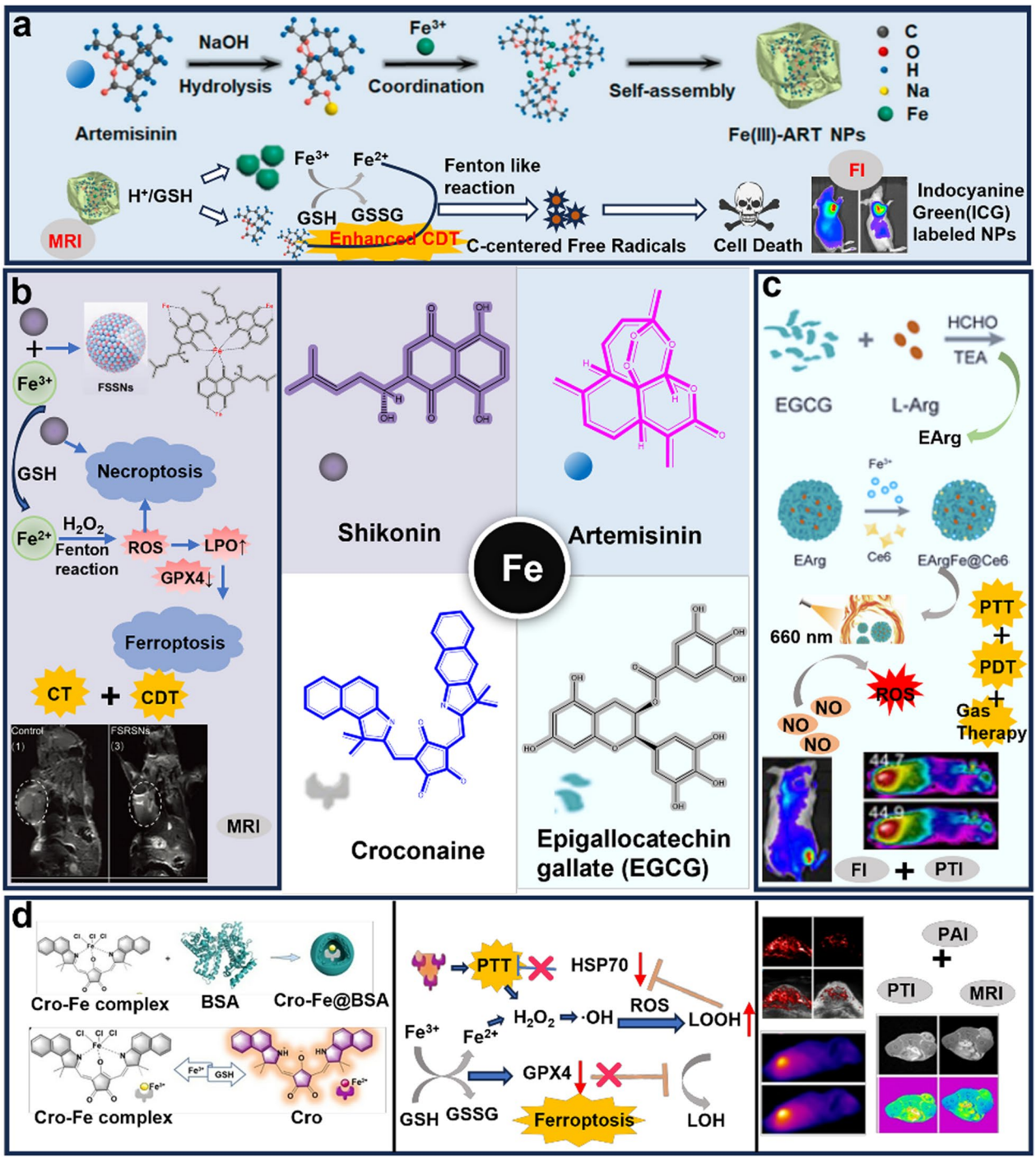

Fig. 3 Some representative natural products coordinated with $Fe^{3+/2+}$. **a** Carrier-free nanoparticles composed of Fe^{3+} coordinated with ART amplify therapeutic strategies for oxidative stress and MRI/FI function. Copyright 2021, Elsevier. **b** Formation of nanoparticles by shikonin and Fe^{3+} through coordination-induced self-assembly for combined CT/CDT as well as MRI. Copyright 2021, Elsevier. **c** The synthesis, mechanism, treatment and bioimaging of EGCG-coordination Fe^{3+} loaded L-Arg. Copyright 2023, Wiley. **d** Fe^{3+}-coordinated croconaine nanoparticle encapsulated with bovine serum albumin was designed for combined PTT and ferroptosis. Copyright 2022, German Chemical Society

of FSP1 and GPX4 was significantly reduced and that of ACSL4 was increased in App-Fe nanocomplex-treated cells, demonstrating that it induced the occurrence of ferroptosis in the cells. Moreover, the release of DAMPs remodeled the TME and enhanced the therapeutic effect of the treatment of tumor [51]. Currently, nitric oxide (NO) was considered as enhancing the therapeutic effects of PTT and PDT on tumors. Therefore, Shi et al. constructed a new strategy, which based on EGCG and Fe3 + coordination to load the NO donor L-arginine (L-Arg) and Ce6 for synergistic PDT/gaseous/PTT (Fig. 3c) [52]. Also using EGCG, in recently published research in June 2024, Li et al. constructed a yeast microcapsule-carrying potent reactive oxygen modulator that can be used as a novel oral drug delivery system targeting the colon. This was done by encapsulating curcumin in a self-assembled manner into a metal-polyphenol network formed by the complexation of EGCG with Fe^{3+}, and then using yeast microcapsules for piggybacking, which cleverly repaired the intestinal microenvironment through the triple pathway of antioxidant, inhibition of inflammation, and regulation of intestinal flora [53]. In addition, Deng et al. also constructed a metal polyphenol network (MPN) using Fe^{3+} and EGCG and loaded CeOx antioxidant nanoenzymes into it to form MPN@CeOx complex nanomaterials. This nanocomposite has excellent targeting as well as MRI functionality. EGCG and CeOx nanoenzymes together scavenge ROS, conferring anti-inflammatory and antioxidant roles to MPN@CeOx, which provides a new strategy of research for the integrated study of the diagnosis and treatment of colonic inflammation [54].

In one study, Fe^{3+}-coordinated croconaine nanoparticle encapsulated with bovine serum albumin (Cro-Fe@BSA) was designed for combined photothermal and ferroptosis cancer therapy. Fe^{3+}were reduced to Fe^{2+} in TME with lower pH and higher GSH concentrations. At the same time, croconaine was released and dispalyed photothermal properties under near infrared irradiation. Elevated temperature increased the rate of the Fenton reaction, leading to enhanced free radical formation. The formation of free radicals in turn prevented the formation of heat-induced heat shock proteins, thereby blocking the self-protection mechanism of cancer cells against heat. It worth notice that the activatable PAI and MRI properties of Cro-Fe@BSA NPs enable the cancer treatment safer and more reliable (Fig. 3d) [55].

Besides the above-mentioned natural products, there were several other components that coordinated with Fe^{3+} and featured multi-pathway therapeutics and multimodal imaging as well. For example, quercetin [56], cinnamaldehyde [57], gossypol [58], Small interfering RNA (SiRNA) [59], were able to coordinate with $Fe^{3+/2+}$. Representative natural products coordinated with $Fe^{3+/2+}$ were summarized in Table 2.

Natural product-coordinated $Cu^{+/2+}$ self-assembly

Copper is an essential micronutrient that exists in the body mainly in the form of copper-protein complexes, which are involved in a wide range of fundamental biological processes. Copper acts as a key catalytic cofactor in a wide range of biological processes, including mitochondrial respiration, oxidative stress, and synthesis of biological compounds. Cu-coordinated compounds have promising applications as potential therapeutic agents [81].

Paclitaxel (PTX) and DOX have been widely used in the clinical treatment of tumors, and Cu^{2+} could be introduced to coordinate with them to achieve better therapeutic effects. As early as the 1980s, it was demonstrated that Cu^{2+} could coordinate with DOX, the Cu-DOX complex could induce tumor cell death by generating ROS, damaging DNA strands, and lipid peroxidation [82]. Zheng et al. prepared a GSH-responsive nanomedicine (COMBO) by coordinating Cu^{2+} with Morusin and DOX through coordination and π-π stacking effects. Their design was that the released Morusin induced paraptosis when COMBO reached the tumor site, while DOX also exerted caspase apoptotic pathway chemotherapeutic effects. To make it easier for the nanomedicine to enter the tumor cells, they synthesized COMBO with an average particle size of 97.85 nm and a uniform dispersion. The different optical phenomena produced by the coordination of Cu^{2+} with Morusin and DOX proved that the coordination was successful, they also demonstrated that the coordination-assembled nanoparticles exhibited higher tumor cytotoxicity and biosafety by cell proliferation and toxicity analysis and Hematoxylin and Eosin stains. This strategy achieved the purpose of paraptosis/CT combination for tumor treatment and effectively overcame tumor resistance [83].

Besides DOX, there were other chemotherapeutic agents that could be coordinated with Cu^{2+} to achieve antitumor effects. Chen et al. chose a widely used proteasome inhibitor ixazomib (IXZ) as ligand to coordinate with Cu^{2+}, then encapsulated Disulfiram (DSF) to form the nano-formulation, which had excellent biosafety and anti-tumor effects [84]. Axitinib (AXB) is an antitumour drug commonly used in renal cell carcinoma, Ji et al. constructed Cu-AXB NPs by simple steps such as stirring and dialysis. Specifically, the amino, carbonyl, and sulphur groups in the AXB structure could form coordination bonds with Cu^{2+} to mediate the self-assembly of the nanoparticles, and the nanoparticles were activated and released by acidic pH after reaching the tumour site, combined with CT /CDT for the treatment

Table 2 Representative natural products coordinated with $Fe^{2+/3+}$

NO	Natural Products	Metal ions	Preparation	TME Response	Size	Treatment	Bioimaging	Reference
1	Dopamine, DA	Fe^{3+}	Mixing	pH, GSH	204 nm	CT/CDT/PTT	——	[39]
2	Tannic acid, TA	Fe^{3+}	–	pH	95.6 nm	CT/PTT	MRI	[33]
3	Tannic acid, TA	Fe^{3+}	Stirring and Ultrasound	pH, ATP	121.17 nm	CT/PTT	PAI/MRI/PTI	[32]
4	Tannic acid, TA	Fe^{3+}	–	ATP	257 nm	CDT/CT	PAI/FI	[35]
5	Tannic acid, TA	Fe^{3+}	–	NIR	> 200 nm	PTT	MRI/PTI	[31]
6	Ellagic acid, EA	Fe^{3+}	Magnetic stirring	TME	25 nm	PTT	PAI/MRI	[38]
7	Porphyrin	Fe^{3+}	Stirring	pH, GSH	145 ± 20 nm	CDT/PDT	FI/MRI	[41]
8	Hematoporphyrin monomethyl ether, HMME	Fe^{3+}	Magnetic stirring	pH, US	~ 70 nm	CT	MRI	[42]
9	Gallic acid, GA	Fe^{3+}	–	pH	110 nm	CT/PTT	MRI	[36]
10	Artemisinin, ART	Fe^{3+}	Magnetic stirring	pH, GSH	80 ± 8.9 nm	CT/CDT	MRI	[44]
11	Tartaric acid, TA	Fe^{3+}	Magnetic stirring	pH	~ 125 nm	CDT/PTT	PTI	[60]
12	Tannic acid, TA	Fe^{3+}	–	–	260.13 ± 1.86 nm	PTT/ICD	PTI	[34]
13	Tannic acid, TA	Fe^{3+}	–	pH, ATP	< 500 nm	CT/PTT	–	[61]
14	Tannic acid, TA	Fe^{2+}	–	pH	–	CT	–	[45]
15	Doxorubicin, DOX	Fe^{3+}	–	pH	–	CT	–	[15]
16	Gallic acid, GA	Fe^{3+}	–	pH	200 nm	CT/CDT	MRI/PTI	[37]
17	Baicalein	Fe^{2+}	Stirring	——	160 nm	CDT/PTT	–	[62]
18	Epigallocatechin-3-gallate, EGCG	Fe^{3+}	Magnetic stirring	pH	~ 100 nm	CT/CDT	FI/MRI	[46]
19	Gallic acid, GA	Fe^{3+}	——	pH	200 nm	CT/CDT	–	[63]
20	Dopamine, DA	Fe^{3+}	Magnetic stirring	pH	60 nm	PTT	PAI/PTI	[40]
21	Pemetrexed, PEM; pseudolaric acid B, PAB	Fe^{3+}	Coordination-driven co-assembly	pH	100 nm	CT	MRI/FLI	[43]
22	Shikonin	Fe^{3+}	Magnetic stirring	GSH	48.2 ± 5.4 nm	CT/CDT	MRI	[47]
23	Quercetin, QU; methotrexate, MTX	Fe^{3+}	Magnetic stirring	pH	181 ± 2 nm	ICD/CT	FI	[56]
24	Gallic acid, GA	Fe^{2+}	–	pH	210.1 nm	CT/CDT	FI	[64]
25	Hematoxylin, HMT	Fe^{3+}	In vivo self-assembly	–	–	PTT/ICD	PTI	[65]
26	SiRNA	Fe^{2+}	Quick ultrasonic	pH	180 nm	CT/CDT	MRI	[59]
27	Polyaminopyrrole, Py-NH2	Fe^{3+}	Magnetic stirring	TME	54.3 nm	PTT	PAI/MRI	[66]
28	GAPDH SiRNA	Fe^{2+}	Magnetic stirring	–	–	CDT	FI	[67]
29	Tannic acid, TA	Fe^{3+}	Magnetic stirring	pH	45.0 nm	CT/CDT/IT	MRI	[68]
30	Benzoic acid, TCPP	Fe^{3+}	Stirring	–	245.2 ± 11.2, 58.1 ± 4.8 nm	PDT/CDT	——	[69]
31	Green tea polyphenols, GTP	Fe^{3+}	Ultrasonic	pH	274 nm	CT/PTT/IT	——	[49]
32	Croconaine	Fe^{3+}	——	GSH/pH	91.3 ± 10.4 nm	PTT/CDT	PAI/PTI	[55]
33	Doxorubicin, DOX	Fe^{2+}	Magnetic stirring	pH/H_2O_2	~ 110 nm	CT/CDT/ICD	FI	[70]
34	Cinnamaldehyde, CA; DOX	Fe^{3+}	Magnetic stirring	pH/H_2O_2	~ 100 nm	CT/CDT	–	[57]
35	Doxorubicin, DOX	Fe^{3+}	Magnetic stirring	pH	77.3 ± 5.3 nm	CT	–	[71]
36	Hyaluronic acid, HA	Fe^{3+}	Magnetic stirring	pH	225 nm	PTT	PAI	[72]
37	Artemisinin, ART; TiO_2	Fe^{3+}	Magnetic stirring	——	170 ± 20 nm	SDT/CDT	–	[73]
38	Amino acids	Fe^{3+}	——	TME	100–140 nm		–	[74]
39	Gallic acid, GA; 5-fluorouracil	Fe^{3+}	Magnetic stirring	DFO	139 nm	CT/PTT	PAI/PTI	[50]

Table 2 (continued)

NO	Natural Products	Metal ions	Preparation	TME Response	Size	Treatment	Bioimaging	Reference
40	Epigallocatechin gallate, EGCG	Fe^{3+}	Magnetic stirring	pH	123.7 nm	PTT/CDT/CT	FI	[75]
41	Epigallocatechin gallate, EGCG	Fe^{3+}	Magnetic stirring	TME	240 nm	PTT/PDT/	FI/PTI	[52]
42	Tannic acid, TA	Fe^{3+}	Magnetic stirring; Ultrasonic	pH	200 nm	CDT/ICD	FI	[76]
43	Polydopamine, PDA	Fe^{3+}	Magnetic stirring	hyperthermia/pH	129.1 ± 6.6 nm	CDT/PTT	FI/PTI	[77]
44	DNAzyme	Fe^{3+}	Vortex	pH	200 nm	CDT/CT	FI	[78]
45	Gossypol	Fe^{3+}	Solvothermal Decomposition	pH/laser	~60 nm	CT/PTT	FI/MRI	[58]
46	Lenvatinib, Adriamycin	Fe^{3+}	–	pH	121 ± 3.74 nm	CT/ICD	FI	[79]
47	Apigenin	Fe^{3+}	Magnetic stirring	pH/GSH	264.7 ± 56.2 nm		FI/MRI	[80]

of aggressive cancers (Fig. 4a) [85]. In addition, Cu^{2+} could also drive the assembly of broad-spectrum chemical drug 5-hydroxy-p-naphthoquinone (HND) and Evans Blue (EB) into nanoparticles. The EB not only stabilizes the nanoparticles but also acts as a tracer for fluorescence imaging. After reaching the tumor site, the acidic microenvironment and endogenous GSH can rupture the nanoparticles to release the drug, in which Cu^{2+} reacts with endogenous GSH and H_2O_2 to generate ROS, and HND not only exerts the effect of chemotherapy, but also amplifies the endogenous H_2O_2 through intracellular oxidoreductase to amplify the oxidative stress in a cascade on-demand together with Cu^{2+} (Fig. 4b) [86].

Huang et al. developed a novel diethyldithiocarbamate (DDTC) nanoparticle loaded with ultrasmall CuS nanodots (CuS NDs), which is triggered by laser to release Cu^{2+}, and has photothermal and ROS-generating functions, synergizing the chemotherapeutic effects of DDTC to jointly fight tumours. Meanwhile, this nanoparticle also has the function of photoacoustic imaging, which provides a guidance for its application (Fig. 4c) [87]. Guo et al. reported the synergistic PDT/CDT/CT triple therapy effect of mesoporous silica nanoparticles (MSNs) delivering methylene blue (MB) and DOX, the outermost layer of MSNs achieves pH-responsive release by coordination with Cu^{2+} and immobilization with DOX to achieve CDT and CT. Combining all three treatment modalities for tumors provides favorable results for cutaneous melanoma [88]. Xiong et al. synthesized a TME-activated nanoplatform using a one-pot method, where hydroxyethyl starch prodrug (HES-SS-DOX) and DA were coordinated and aggregated into nanoparticles via Cu^{2+}, in which Cu^{2+} acted as a bridge to connect DA and DOX. After reaching the tumor site and cleavage, DOX exerted CT, while Cu^{2+} acted as CDT, and the coordination and aggregation makes the near-infrared absorption of PDA significantly enhanced, which strengthen the PTT effect (Fig. 4d) [89].

CDT, which uses Fenton action catalysts to kill cancer cells by converting intracellular H_2O_2 into toxic ·OH, has a promising application in tumor therapy. Among the various metal-mediated Fenton-like reactions, those involving $Cu^{+/2+}$ showed higher reaction rates than other metal ions under weakly acidic conditions. Theoretically, the Fenton catalytic efficiency of Cu-based nanoplatforms is about 160 times higher than that of conventional iron-based reagents. An efficient hierarchical structured nanoplatform with transferrin-labeled Cu-oxide dot-decorated $Cu@Gd_2O_3$ was designed to act as a GPX4 antagonist and a SOD-1 agonist, leading to intracellular ROS and H_2O_2 accumulation. Self-supply of Cu^{+} was achieved by utilizing the ratio of CuO to elemental Cu nuclei, which catalyzed the formation of ·OH from H_2O_2 [90]. CDT is difficult to achieve favorable results if it only relies on endogenous H_2O_2 in tumor cells. A therapeutic strategy that could simultaneously inhibit enzyme activity and amplify CDT was proposed: a thioglycolic acid (TGA)-Cu coordinated nanoparticle with a fast response to GSH was synthesized to enhance CDT efficiency, at the same time the oxidized glutathione (GSSG)-Cu complex triggered oxidative stress of H_2O_2 to prompted tumor cell death [91]. Multi-modality combination therapy alleviates the drawbacks of monotherapy and demonstrates better treatment effects. For example, hollow mesoporous silica nanoparticles (HMSNs) were utilized as carriers and loaded with the complexes of Cu^{2+} and PDA to form nanoparticles. Among them, the photothermal performance of PDA was further improved by its coordination with Cu^{2+}; the temperature increase induced by PTT further increased the CDT efficiency,

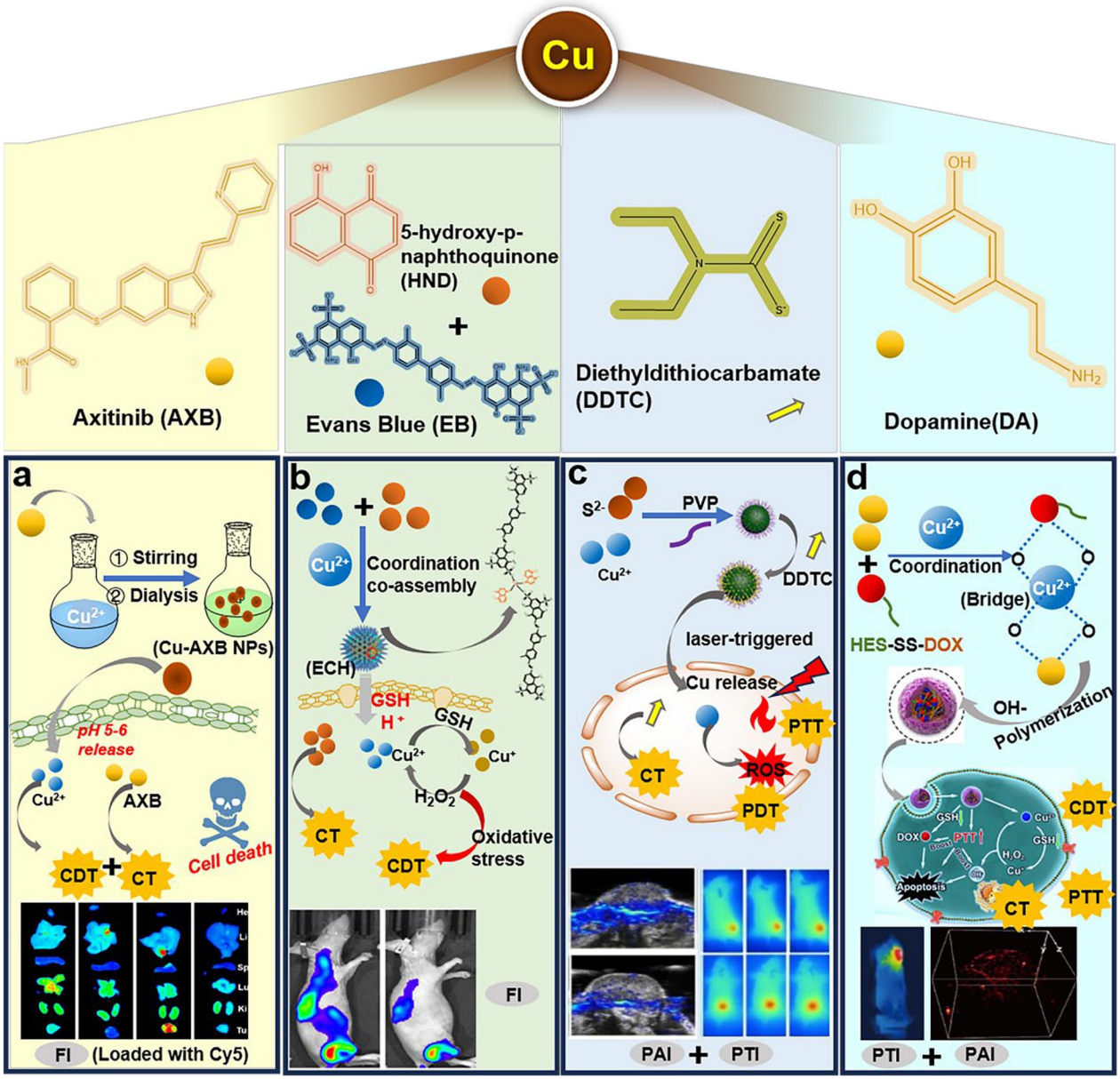

Fig. 4 Some representative natural products coordinated with Cu^{2+}. a) Methods of Axitinib coordination with Cu^{2+}, response to acidic pH release, and treatment strategies. Copyright 2023, Royal Society of Chemistry**.** b) Coordination of Cu^{2+} with EB/HND and TME responsive release. Copyright 2023, Royal Society of Chemistry**.** c) CuS NDs assembled by PVP and combined with DDTC to achieve a combined CT/PDT/PTT strategy and PAI/PTI functions. Copyright 2020, American Chemical Society. d) Cu^{2+}-driven coordination and assembly aggregation of DOX and DA to achieve CDT/PTT and PAI functions. Copyright 2022, Ivyspring International Publisher

thus realizing the synergistic effect of the two modes of PTT/CDT [92]. Similarly, Liu et al. used a Cu^{2+}-triggered coordination strategy to assemble Cu^{2+} and Indocyanine Green (ICG) with tirapazamine (TPZ) to form Cu-ICG/TPZ NPs. The Cu-ICG/TPZ NPs would aggregate at the tumor site through the enhanced permeability and retention (EPR) effect. The hypoxia of the TME would trigger the CT effect of the TPZ, Cu^{2+} and ICG would play the roles of CDT and PDT, respectively, resulting in a synergy with the Synergistic tumor therapy with three therapeutic modalities [93].

Flavonoids and polyphenols due to their benzene ring and the oxygen atom on the carbonyl group to form a large π-bond conjugate system, the oxygen atom of the carbonyl group in the C ring has a strong coordination ability. It can be coordinated with ions of trace metal

elements to form stable flavonoid complexes, such as TA, curcumin and cardamonin that have been coordinated with Cu^{2+} for the treatment of tumors. For example, Sun et al. coordinated Cu^{2+} with TA then encapsulated by phycocyanin (PC), Zn^{2+}, disulfide-bonded cross-linking agent and HA to constitute stable flavonoid composite nanocapsules (PZTC/SS/HA). The principle of their experiment was that the PZTC/SS/HA could be activated by TME to cleave and release Cu^{2+}, followed generation of Cu^{2+} sulfide (CuS) for PTT by endogenous H_2S-triggered. In addition, PTT and Cu^{2+} could activate and enhance CDT. To demonstrate the pH/GSH response of PZTC/SS/HA, the results in different solutions show that the PZTC/SS/HA collapsed the most completely and released Cu^{2+} faster in the acidic environment and the simultaneous presence of GSH. The prepared PZTC/SS/HA showed concentration- and power-dependent photothermal effects under 1064 nm laser irradiation. Their TME-activated synergistic PTT/CDT strategy showed promising therapeutic effects, opened new avenues for the generation of novel nano-agents and effective TME-responsive synergistic treatment of cancer [94]. Cardamonin is a polyphenolic natural product that is cytotoxic to a variety of cancer cells. It has been reported that the complex formed by Cu^{2+} and cardamonin could induce apoptosis in cancer cells by inducing DNA damage and generating ROS, its biological activity was verified on MDA-MB-468 and PANC-1 cells [95]. Naringenin is a widely distributed flavonoid compound with antioxidant and antitumor effects. The formation of a triple component complex with Cu^{2+} and naringenin (Nar) using bartophenanthroline as a ligand showed high selectivity and toxicity against A549 cells [96]. Emami et al. synthesized a Cu^{2+} complex of curcumin and 2,2'-bipyridine-5,5'-dicarboxylic acid, which was highly cytotoxic to the cancer cell line MDA-MB-231 and safe for normal cells [97]. Cu^{2+} was coordinated with shikonin then added DTC-PPB to become NPs, the NPs could be cleaved by ROS, the released DTC rapidly chelate Cu^{2+} to synthesize highly cytotoxic $Cu(DTC)_2$ and induce the release of DTC-PPB, which in turn ROS could be generated to release a positive feedback activation loop to further activation. Thus, this nano-amplifier could be triggered by ROS in the TME to develop a cascade-amplified positive feedback loop in-situ to enhance the therapeutic efficacy of tumor treatment [98].

Also utilizing the TME response, Zhu et al. designed a self-delivery nanomedicine assembled from Cu^{2+} coordination-driven celastrol and ICG. The nanomedicine were wrapped with red blood cell membranes (RBCs) to prolong the drug's circulation time and activated by GSH in TME to exert the combined therapeutic effect of CT/PTT/CDT [99]. Similarly, a Cu^{2+}-coordinated nano-formulation utilizes Cu^{2+} to drive the assembly of the photothermite ICG and the photodynamic agent pheophorbide A (PhA). It could be decomposed by acidic pH and high GSH in TME, then Cu^{2+} could consume GSH to catalyze ROS production. Meanwhile, after fluorescence and photoacoustic imaging-guided NIR irradiation given at different wavelengths, ICG and PhA played the roles of PTT and PDT, respectively, to induce apoptosis of tumor cells (Fig. 5a) [100]. Likewise, a hydrogel composed Cu^{2+} with ICG and HA could also function as a PTT/CDT under NIR [101]. Cu^{2+} also could be assembled with cy series dyes in a coordination-driven manner, followed by encapsulation with HA to form nanoparticles with synergistic PTT/CDT dual therapeutic modes. A strong anti-tumor effects could be achieved at low doses [102].

In addition to common therapeutic modalities such as PTT/CDT/CT, immunogenic cell death (ICD) was also a popular research topic. Cu^{2+}, DOX, and NLG919 could self-assemble by coordination through π-π stacking effect to form a nanoscale oxidative stress amplifier (called Cu-DON). It could effectively aggregate at the tumor area, release DOX under GSH to initiate immunogenic chemotherapy (IC). Meanwhile, Cu^{2+}-triggered oxidative stress enhancement disrupted the intracellular redox homeostasis, leading to ICD. Dual immunotherapy effectively inhibited the growth of primary and distal tumors, providing a new direction for clinically blocking tumor growth and metastasis (Fig. 5b) [103]. Cu^{2+} was coordinated with linoleic acid hydroperoxide (LAHP) to synthesize NPs, the NPs were brought to the tumor site with R7-modified iRGD peptide. Under the acidic pH of TME, the decomposition into LAHP and Cu^{2+} produced ROS and further induced ICD [104]. Wang et al. constructed a mixed-valent Cu^{2+} coordination nanopolymer: 5'-guanosine monophosphate (5'-GMP), which is widely present in organs, and then self-assembled into Cu-NCPs with a particle size of about 100 nm. The valence state jump of the coordinated, partial conversion of Cu^{2+} to Cu^{+} enhanced RT-mediated oxidative stress, which in turn induced the release of potent ICD and tumor-associated antigens and DAMPs. Cu-NCPs significantly facilitated T-cell infiltration, thereby enhancing the radioimmunotherapy of in situ and metastatic tumors [105]. Accumulation of intracellular $Cu^{+/2+}$ triggers aggregation of mitochondrial lipidated proteins and destabilization of Fe-S cluster proteins, leading to a novel type of regulated cell death distinct from oxidative stress-associated cell deaths (e.g., apoptosis, Ferroptosis and necrotic apoptosis), called Cuproptosis [106]. A Cu^{2+}-mediated self-assembly of glycyrrhizic acid and nortriptyline (NCTD) into a carrier-free natural small-molecule water gel-for-injection by coordination and hydrogen bonding. It could

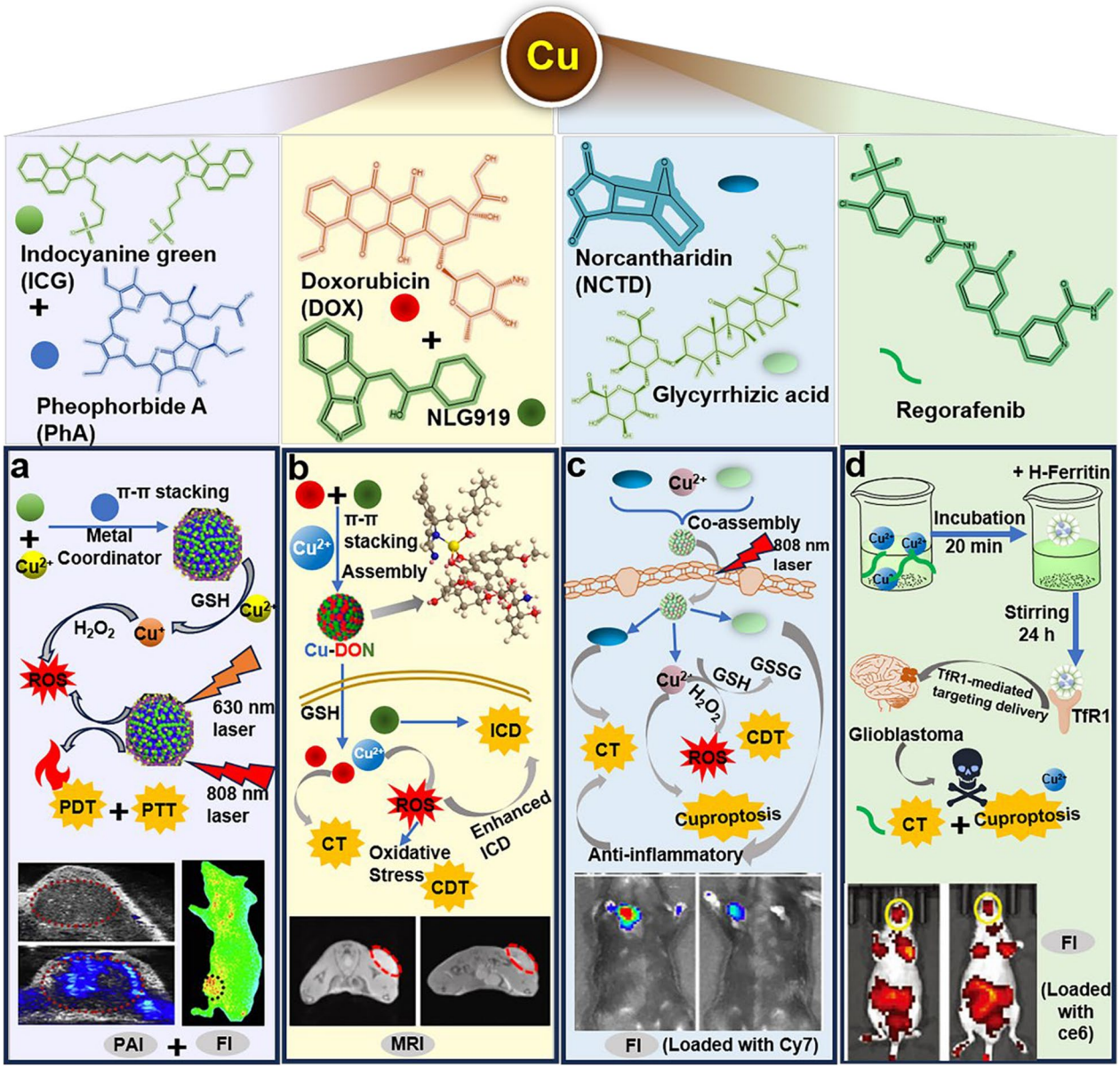

Fig. 5 Some representative natural products coordinated with Cu^{2+}. **a** Cu^{2+} with ICG and PhA via coordination for PDT/PTT combination and PAI/FI combination. Copyright 2021, Elsevier. **b** Cu^{2+}, DOX, and NLG919 self-assembly for ICD and MRI. Copyright 2021, Elsevier. **c** Cu^{2+}-mediated self-assembly of glycyrrhizic acid and NCTD into carrier-free natural injectable small-molecule hydrogels activates CDT/CT/Cuproptososis via NIR. Copyright 2023, Elsevier. **d** Cu^{2+} coordinated regorafenib and encapsulated with H-ferritin (HFn) to obtain brain-targeted nanoparticles for synergistic treatment of glioblastoma. Copyright 2023, Wiley

consume GSH to generate ROS under NIR and synergistically regulate TME through apoptosis, CDT, Cuproptosis and anti-inflammation. The gel composition is the active component of traditional Chinese medicine, the preparation process was simple. The carrier-free protein drug generated by the coordination of natural products with $Cu^{+/2+}$ has a brilliant prospect of application in the treatment of tumors (Fig. 5c) [107]. Jia et al. incubated Cu^{2+} with regorafenib for 20 min and then added H-ferritin (HFn) and stirred for 24 h to obtain brain targeted nanoparticles. HFn as a TfR1 targeting agent, could reach the glioblastoma site and release regorafenib in response to acidic pH, leading to cellular autophagy. In addition, the increase of intracellular Cu^{2+} played a role in Cuproptosis, CT/Cuproptosis synergistically treats glioblastoma (Fig. 5d) [108].

Metal–organic complexes (MOCs) or metal–organic frameworks (MOFs) possess a great deal of attraction in nanodrug delivery systems for tumors. As an emerging porous material with organic–inorganic hybridisation, MOFs have high specific surface area and porosity compared with traditional drug delivery systems, which is conducive to effective encapsulation and delivery of various drugs. Their toxicity can also be regulated by selecting suitable metal ions, so that MOFs have sufficient stability and low biotoxicity in organisms [109, 110]. They have been applied in energy storage, catalysis, sensing, bio-imaging, drug delivery and so on [111, 112]. Metal ions coordination-driven composite systems enabled stable delivery of specific drugs in response to physiological conditions. Li et al. utilized the metal-coordination interaction of Cu^{2+} with PPEIDA and DOX to construct a pH-sensitive nanoparticles. Its excellent targeting and pH sensitivity enabled real-time monitoring of drug loading and release [113]. A highly efficient mitochondria-targeted photosensitizers with aggregation-induced release (AIE) characteristics for effective PDT by using a Cu^{2+}-based metal–organic framework MOF-199 was synthesized, it showed excellent mitochondri-targeting ability and specific ablation of cancer cells under NIR irradiation [114]. A dual-loaded nanodrug based on metal–organic particles with Cu^{2+} as a ligand bridge connecting Combretastatin A4 (CA4) and Mitoxantrone (MIT) to obtain CMMOP. CMMOP was relatively stable under normal physiological conditions and cleaves under the acidic pH of tumors to release the drug, providing good performance for precision therapy [115].

In addition to inorganic $Cu^{+/2+}$, Copper oxide nanoparticles and organic forms of $Cu^{+/2+}$ complexes could also be used to synthesize cytotoxic anticancer drugs, leading to irreversible membrane damage and cell death. For example, the combination of CuO NPs with N-acetylcysteine generates ROS while interfering with the cell membrane and caspase-independent cell death [116]. An emerging therapeutic approach for CO gas therapy has been extensively investigated. Sun et al. used a coordination assembly strategy to synthesize Cu^{2+}-flavonoid coordination polymer nanopredrug. This nanopredrug was relatively stable, when it reached the tumor site, a large quantity of GSH in the TME would break the coordination bond, causing the release of Cu^{+} and free Fle. Cu^{+} was used to react with H_2O_2 to exert CDT; NIR breaks the C–C bond and releases CO to exert gas therapy [117]. Representative natural products coordinated with $Cu^{+/2+}$ were shown in Table 3.

Natural product-coordinated $Mn^{2+/3+}$ self-assembly

$Mn^{2+/3+}$ is an essential trace element for living organisms and distributed in various tissues and body fluids. It plays a positive role in the growth and development of bones and the improvement of muscle hematopoiesis. In addition, $Mn^{2+/3+}$ can promote the survival and proliferation of immune T-cells and effectively propel the tumor-killing ability of NK cells [131, 132]. Currently, extensive research showed that natural products coordinated with $Mn^{2+/3+}$ would offer an excellent PTT, CDT and immune effect. They could be also utilized for PAI, MRI and PTI due to the paramagnetic properties [133, 134].

Immunotherapy has emerged as an effective strategy for the treatment of cancer. Numerous studies have reported $Mn^{2+/3+}$-mediated immune responses [135]. In this aspect, Geng et al. self-assembled Mn^{2+} with DOX and Ce6 into highly drug-loaded nanoparticles, which were further encapsulated with erythrocyte membranes to improve the dispersion and stability of the nanoparticles. It indicated that the encapsulated nanoparticles enhanced the anti-tumor response of primary and distant tumors, providing a new approach for immunotherapy (Fig. 6a) [136]. Liu et al. reported an innovative strategy for inhibiting heat shock proteins to improve PTT efficiency: GA and Mn^{2+} coordinated through stirring to form nanoparticles. Degradation under acidic conditions releases $Mn^{2+}$and GA, leading to upregulation of ROS, mitochondrial dysfunction, and pyroptosis. The reduction of ATP and accumulation of ROS during this process provide a powerful method for inhibiting heat shock proteins expression, making it possible for mild PTT mediated by nanomaterials (Fig. 6b) [137]. In addition, Yan et al. reported a nanoplatform via Mn^{2+} coordinated and self-assembled with CDN STING, which effectively delivered STING agonists to immune cells [138]. The amphiphilic PEG-polyphenol was successfully utilized to coordinate with $NaGdF_4$ and Mn^{2+}. This radiosensitizer increased the sensitivity of tumor cells to X-rays and promoted immune cell maturation. In addition, Mn^{2+} could promote STING pathway activation, and the combination of the two therapeutic modalities was interesting for tumor radiotherapy [139]. Dai et al. studied the reversal of the immunosuppressive microenvironment by self-assembling and efficiently loading immunomodulators (R848) with NIR-II semiconductor polymer dots and Mn^{2+}. They skillfully assembled the function of FI, PAI, PTT and CDT in nanoparticles. In addition, the nanoparticles catalyzed the generation of ·OH from H_2O_2 leading to a decrease in the absorption peak of MB, proving that it had promising CDT effects [140].

The combination of gene therapy and CT provides an effective solution for tumor treatment. TA coordinated with Mn^{2+} to form a high-loading carrier for the effective co-delivery of rapamycin (RAP) and Beclin-1 to achieve inhibition of Deoxyribozyme (DNAzyme, DZ) [141]. Similarly, in another study, Mn^{2+} coordinated with

Table 3 Representative natural products coordinated with $Cu^{+/2+}$

NO	Natural products	Metal ions	Preparation	TME Response	Size	Treatment	Bioimaging	Reference
1	Diethyldithiocarbamate, DDTC	Cu^{2+}	Stirring	NIR	~8.8 nm	PTT/PDT/CT	PAI/PTI	[87]
2	Paclitaxel, doxorubicin	Cu^{2+}	Thin-film hydration method	ROS/GSH	128.5 ± 2.610 nm	CDT/CT	–	[118]
3	Indocyanine green, ICG; pheophorbide A, PhA	Cu^{2+}	Stirring	pH/GSH/NIR	~141.6 nm	PTT/PDT/CDT	FI/PAI/PTI	[100]
4	Indocyanine green, ICG; hyaluronic acid, HA	Cu^{2+}	Stirring	pH	–	PTT/CDT	PTI/FI	[101]
5	Cardamonin	Cu^{2+}	–	–	–	CT/CDT	–	[95]
6	poly(p-phenylene ethynylene) backbone and iminodiacetic acid (IDA), PPEIDA; DOX	Cu^{2+}	Stirring	pH	~171.7 nm	CT	–	[113]
7	Hyaluronic acid, HA; fluorescence dye, Cy	Cu^{2+}	Stirring	GSH	~100 nm	CDT/PTT	FI/PTI	[102]
8	3-hydroxy-4′-carboxyl flavone (Fle)	Cu^{2+}	Sonicated	NIR/GSH	~150 nm,	CO/CDT	–	[117]
9	N-acetylcysteine	Cu^{2+}	–	–	~80 nm	CT	–	[116]
10	5′-guanosine monophosphate, 5′-GMP	Cu^{2+}	Stirring	Ionizing radiation	100 ± 7.48 nm	radioimmunotherapy/CDT	–	[105]
11	Apoferritin	Cu^{2+}	Stirring	pH	~20 nm	Autophagy-dependent apoptosis, CT	–	[119]
12	Polydopamine, PDA	Cu^{2+}	Magnetic stirring	NIR	~130 nm	CDT/PTT	–	[92]
13	Doxorubicin, NLG919	Cu^{2+}	Magnetic stirring		139.3 ± 0.6 nm	ICD/CDT	MRI	[103]
14	Morusin; Doxorubicin, DOX	Cu^{2+}	Mixed centrifugal resuspension	GSH	97.85 ± 0.42 nm	PCD/CT	–	[83]
15	Naringenin, Nar	Cu^{2+}	–	–	–	CDT/CT	–	[96]
16	Thioglycolic acid, TGA	Cu^{2+}	self-assemble	GSH	~43.8 nm	CDT	–	[91]
17	Ixazomib, IXZ	Cu^{2+}	Reversed-phase microemulsion method, stirring	GSH	–	CT	FI	[84]
18	Curcumin,Cur; 2,2′-bipyridine-5,5′-dicarboxylic acid, BPYD	Cu^{2+}	–	–	–	CT	–	[97]
19	Doxorubicin, DOX	Cu^{2+}	Stirring	pH, NIR	~100 nm	PDT/CDT/CT	–	[88]

Table 3 (continued)

NO	Natural products	Metal ions	Preparation	TME Response	Size	Treatment	Bioimaging	Reference
20	Phosphorus dendrimer-copper (II) complexes (1G (3) -Cu)	Cu^{2+}	Stirring	TME	~210 nm	ICD/CT	MRI	[120]
21	Shikonin	Cu^{2+}	Stirring	ROS	~120 nm	CT	FI	[98]
22	Tirapazamine; ICG	Cu^{2+}	Ultrasound, Stirring, dialysis	GSH, Hypoxia	~150 nm	CT/CDT/PDT	FI/PTI	[93]
23	Amphiphilic amino acids; glucose oxidase, GOx; doxorubicin, DOX; camptothecin, CPT	Cu^{2+}	–	TME	–	CT/CDT	–	[121]
24	Linoleic acid hydroperoxide, LAHP	Cu^{2+}	Stirring	pH	~100 nm	PDT/ICD	–	[104]
25	Combretastatin A4, CA4; mitoxantrone, MIT	Cu^{2+}	–	pH	–	CT	–	[115]
26	Dopamine, DA	Cu^{2+}	Stirring	TME	~171.2 nm	CDT/CT/PTT	PAI/PTI	[89]
27	Celastrol, CST; ICG	Cu^{2+}	Stirring	GSH	~110 nm	CDT/CT/PTT	PTI	[99]
28	Disulfiram, DSF; mitoxantrone, MTO	Cu^{2+}	Stirring, ultrasonically disperse	pH	~110 nm	CT/CDT	–	[122]
29	Gallic acid, GA	Cu^{2+}	Stirring, hydration	GSH	~50 nm	PTT/CDT	PTI	[123]
30	Tannic acid, TA	Cu^{2+}	Magnetic stirring	TME	~133.5 nm	PTT/CDT	PTI	[94]
31	Glycyrrhizic acid, GA; norcantharidin, NCTD	Cu^{2+}	Magnetic stirring	NIR	–	CDT/CT/cuproptosis	FI	[107]
32	Human H-ferritin	Cu^{2+}	Magnetic stirring	pH	~15.5 nm	cuproptosis/CT	FI	[108]
33	L-cysteine; polyvinylpyrrolidone, PVP	Cu^{2+}	Stirring	pH	~100 nm	CDT/CT	–	[124]
34	Zinc protoporphyrin IX, ZnPPIX	Cu^{2+}	ultrasound-assisted synthesis; Stirring	GSH	178 nm*60 nm	CDT/CT	–	[125]
35	Histidines in ARGD polypeptide	Cu^{2+}	chelation	TME	~60 nm	CT/CDT	FI	[126]
36	Dopamine, DA	Cu^{2+}	Magnetic stirring	pH	~100 nm	CDT/PTT/CT	PAI/PTI	[127]
37	Gum Arabic, GA	Cu^{2+}	Magnetic stirring and shaken in a rotating incubator	pH/GSH	~92.17 nm	CT/CDT	–	[16]
38	Apatinib	Cu^{2+}	–	TME	–	CT/CDT	–	[128]
39	Axitinib	Cu^{2+}	Stirring; dialysis	pH	~180 nm	CT/CDT	FI	[85]

Table 3 (continued)

NO	Natural products	Metal ions	Preparation	TME Response	Size	Treatment	Bioimaging	Reference
40	Evans Blue, EB; 5-hydroxy-p-naphthoquinone, HND	Cu^{2+}	shaking	TME	~200 nm	CDT/CT	FI	[86]
41	Zinc phosphate, ZnP; prussian blue, PB	Cu^{2+}	Stirring	pH	~160 nm	CDT/PTT/CT	PTI	[129]
42	Cinnamaldehyde	Cu^{2+}	–	white LED light irradiation		CDT	–	[130]

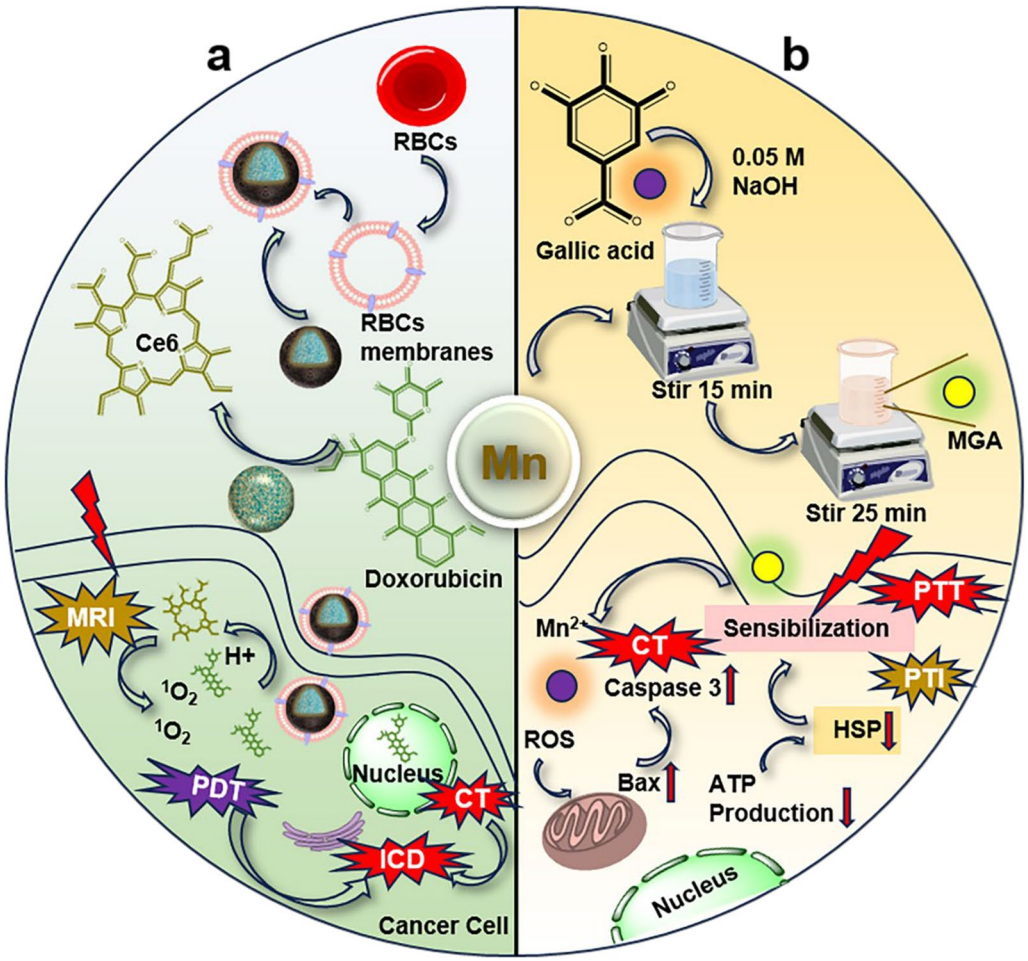

Fig. 6 Some representative natural products coordinated with Mn^{2+}. **a** Mn^{2+} was self-assembled with DOX and Ce6 to form highly drug-loaded nanoparticles and then encapsulated with erythrocyte membrane for ICD. Copyright 2021, Elsevier. **b** GA and Mn^{2+} were coordinated to form nanoparticles and cleaved under acidic conditions to cause CT/PTT. Copyright 2023, springer nature

TA was utilized to deliver the anticancer drug DOX and DNA enzymes with the high drug loading property. Both in vivo and in vitro studies demonstrated that nanoparticles presented satisfactory antitumor efficacy [142]. In addition, Mn^{2+}-mediated imaging technology visualizes tumor therapy. Wu et al. synthesized a pH-responsive multifunctional nanoparticle based on the coordination of methotrexate (MTX) and Mn^{2+}, encapsulating a nanoscale polymer of PEG, in which Mn^{2+} acted as the MRI contrast agent, MTX was as the chemotherapeutic agent, and PEG provided the nanoparticles with a stable environment, respectively. In vivo MRI indicated that nanoparticles exerted favorable anti-tumor effects [143]. Furthermore, Geng et al. designed and developed a GSH-responsive nanoparticle in which Mn^{3+} was coordinated with hematoporphyrin monomethyl ether (HMME) and then loaded with DOX, subsequently modified with a targeted polyethylene glycol polymer to enhance tumor targeting. Nanoparticles ruptured and then Mn^{3+} reduced to Mn^{2+} for PDT and MRI in a high level GSH environment, while DOX was applied for CT. In vivo anti-tumor experiments demonstrated that it significantly inhibited tumor growth and showed a favorable biosafety profile [144]. Mn^{2+} was coordinated with AsO_4^{3-} and ICG to form MnAs-ICG NPs. The chemodynamic property of Mn^{2+}, the chemotherapeutic property of AsO_4^{3-}, and the photothermal property of ICG were fully utilized. In the meanwhile, the presence of Mn^{2+} and ICG allowed the application of MRI and FI [145].

In vivo coordination self-assembly enhanced drug efficacy. A study utilized PEG-modified hollow mesoporous manganese dioxide nanoparticles to load with the antitumor drug bleomycin (BLM). BLM and Mn^{2+} were released in the TME with in situ coordination self-assembly. The antitumor effect of BLM was enhanced, and it could be also employed in MRI to monitor the therapeutic effects in vivo [146]. Overall, the coordination of $Mn^{3+/2+}$ with natural products effectively stimulated the immune response of the body, and demonstrated promising therapeutic effects in PTT and CDT. Meanwhile, the introduction of $Mn^{3+/2+}$ allowed for PAI, PTI and MRI. Representative natural products coordinated with $Mn^{2+/3+}$ were shown in Table 4.

Natural product-coordinated Zn^{2+} self-assembly

Zinc is existed mainly in the form of enzymes and performs an important function in promoting wound healing and bacterial inhibition. It supports coordination in different geometries as well as being able to facilitate ligand exchange [149]. Zinc derivatives are proposed as antitumor agents and numerous Zinc coordination complexes have been synthesized.

Lei et al. assembled zinc-fluorouracil metallodrug networks (Zn-Fu MNs) by one-pot coordination of zinc nitrate and fluorouracil with cleavage of the mitochondrial electron transport chain. Zn^{2+} induced ROS production and 5-fluorouracil interfered with DNA synthesis, both of which synergistically activated immunotherapy (Fig. 7a) [150]. Zn^{2+} could also drive RNA self-assembly to form spherical nanoparticles with excellent RNA loading and bioavailability. The results showed that RNA oligonucleotides with different lengths and

Table 4 Representative natural products coordinated with $Mn^{2+/3+}$

NO	Natural products	Metal ions	Preparation	TME Response	Size	Treatment	Bioimaging	Reference
1	Tannic acid, TA	Mn^{2+}	Stirring	pH, GSH	151 ± 24 nm	GT/CT	FI	[141]
2	Tannic acid, TA	Mn^{2+}	High temperature heating	pH, GSH	~ 230 nm	CDT/GT/CT	FI	[142]
3	Methotrexate, MTX	Mn^{2+}	Sonication	pH	93.3 ± 10.3 nm	CT	MRI	[143]
4	Polydopamine, PDA	Mn^{2+}	Magnetic stirring	–	105 nm	CDT/PTT	MRI/PTI /FI	[147]
5	Hematoporphyrin monomethyl ether, HMME	Mn^{3+}	Mild sonication	GSH	~ 100 nm	CT/CDT/PDT	MRI	[144]
6	Doxorubicin, DOX; chlorin e6, Ce6	Mn^{2+}	Sonication	pH	125 ± 6.1 nm	CT/PDT	MRI	[136]
7	Carrying DNA	Mn^{2+}	–	pH	~ 100 nm	CDT	–	[148]
8	Cyclic dinucleotide, CDN	Mn^{2+}	–	pH	118 ± 41 nm	ICD	–	[138]
9	Indocyanine green, ICG	Mn^{2+}	Magnetic stirring	pH	144.87 ± 2.91 nm	CT/CDT/PTT	FI/MRI	[145]
10	Beomycin, BLM	Mn^{2+}	In Vivo self-assembly	GSH	~ 300 nm	CT	MRI	[146]
11	Resiquimod R848	Mn^{2+}	Stirring	pH	~ 100 nm	PTT/ICD/CDT	FI/PAI	[140]
12	Gallic acid, GA	Mn^{2+}	Magnetic stirring	pH	164.2 nm	PTT	PTI	[137]
13	2-methylimidazole, 2-MI	Mn^{2+}	Magnetic stirring	pH	~ 130 nm	ICD	FI	[135]
14	Banoxantrone; AQ4N	Mn^{2+}	Magnetic stirring	pH	~ 100 nm	CT	PAI	[134]

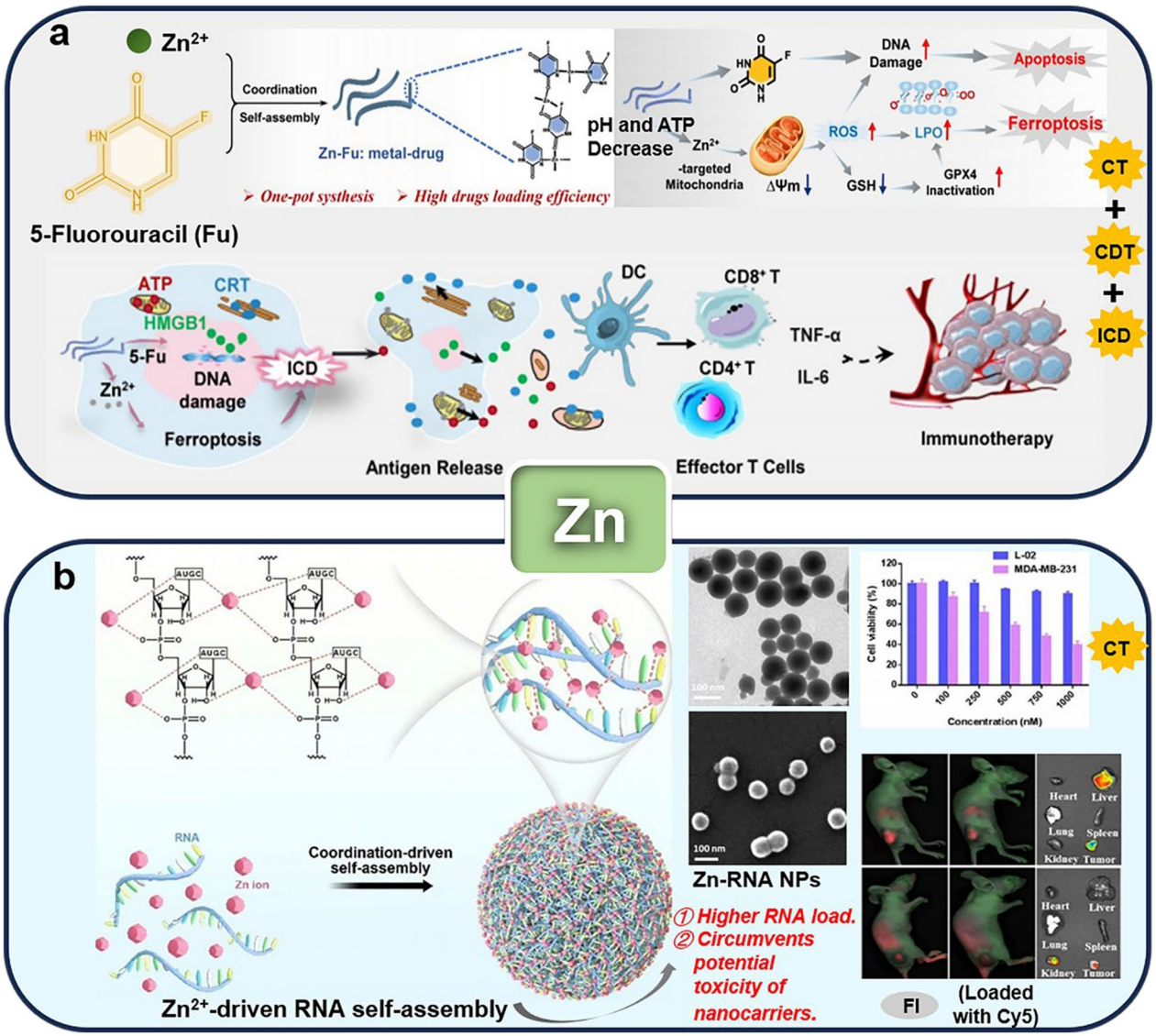

Fig. 7 Some representative natural products coordinated with Zn^{2+}. a) Self-assembly of Zn^{2+} and Fu into metallodrug networks for CT/CDT/ICD combination. Copyright 2022, Ivyspring International Publisher. b) Schematic diagram of Zn^{2+}-driven RNA self-assembly to form spherical nanoparticles. Copyright 2021, Wiley

structures could self-assemble into nanoparticles. This coordinated-induced self-assembly extended the application of RNA therapeutics (Fig. 7b) [151]. Endogenous Zn^{2+} and small biomolecules (l-cystine, Cys) were assembled into a new tumor-sensitive metal–organic complex, and then DOX was encapsulated inside. The nanomedicine was cleaved under the overexpressed GSH in the tumor to release the drug, which showed higher targeting and cytotoxicity than free DOX. Since both metal ions and organic ligands are derived from natural products, it is characterized by favorable biocompatibility, high tumor sensitivity and low toxicity for normal cells [152].

The research and development of coordination-driven metal–organic nanoplatforms provided an effective strategy and direction for treating glioblastoma as well. Gao et al. reported an in-situ assembly nanoplatform based on RGD peptide-modified bisulfite-Zn^{2+}-dipicolylamine-Arg-Gly-Asp and ultrasmall Au-ICG nanoparticles. It could target tumors and waited for ultra-small Au nanoparticles to cross the blood–brain barrier before assembling with them in situ to form a large nanocluster. In situ photothermal therapy by NIR irradiation under FI, MRI and PAI guidance [153]. In fact, mild PTT (42–45 °C) exerted a significant therapeutic effect with less tissue

damage [154]. Combining gene therapy (GT) with mild PTT could inhibit the heat resistance of tumor cells, minimize side effects and improve the overall therapeutic efficacy. A nanoplatform for co-delivery of photothermal and gene therapy agents was developed by self-assembly using a one-pot method. IR780-1 and 2-methylimidazole (2-MIM) were utilized as ligands to coordinate with Zn^{2+} in the presence of siRNA to form a nanoplatform. It was available for PTI, PAI, and FI-guided PTT and GT. At the same time, it overcame the short half-life and instability of drugs in conventional PTT and GT therapy [155]. Representative natural products coordinated with Zn^{2+} were summarized in Table 5.

Natural product-coordinated Co^{3+} self-assembly

Cobalt is a biologically essential trace element usually found in vitamin B12 (vitamin B12, also known as cobalamin, the only vitamin containing the metal element). Its physiological functions are also shown through the actions of vitamin B12, including hematopoietic function, protein metabolism and the synthesis of certain enzymes. Co^{3+} achieved coordination assembly with some natural products for tumor therapy. For example, Co^{3+} and tetrakis (4-carboxyphenyl) porphyrin (TCPP) were assembled into a metal–organic framework (MOF) then coordinated it with mitochondria-targeted triphenylphosphonium (TPP) to construct an ultrasound-responsive nano-agonist TPP@CoTCPP. Due to the deep penetration and non-invasive nature of ultrasound, after the nanosheets entered into the tumor cells and localized in the mitochondria, the ultrasound drived the MOF to generate ROS. It resulted in a precise and controllable stimulation of the cGAS-STING pathway and promoted the immune-suppressing tumors [157]. Representative natural products coordinated with Co^{3+} were displayed in Table 6.

Natural product-coordinated $Mo^{4+/5+}$ self-assembly

Molybdenum, an essential trace element for humans, animals and plants, is naturally present in multiple enzymes. Its complexes are expected to be potential candidates for biomedical applications. Zhen et al. inspired by the game theory, proposed a cancer therapy by combining CDT/ICD, considering the evolutionary, competitive and cooperative relationship between certain molecules and cancer cells. They coordinated Mo^{5+} with EGCG to form a nanoparticle. It eliminated the excess GSH through Michael addition reaction and regulated ROS levels through Fenton-like reactions and the Russel mechanism, thus disrupting the redox balance. Furthermore, the NPs formed aggregates in TME and mechanically disrupting endosomes and plasma membranes to induce ICD. This strategy not only generated ROS by consuming GSH with the introduction of Mo^{5+}, but also induced ICD through competition for intracellular GSH to form larger aggregates, thus facilitating immunotherapy [158]. Yang et al. coordinated PDA with MoS_2 and targeted modification of its surface before loaded DOX to form a multifunctional nanoplatform. The nanoplatform could be monitored by FI, PAI and MRI to effectively aggregate at the tumor site and release DOX under pH/NIR triggering, and the combination therapy of PTT/CT showed excellent tumor cell killing effect [159]. Representative natural products coordinated with $Mo^{4+/5+}$ were displayed in Table 6.

Natural product-coordinated Sn^{4+} self-assembly

Tin plays a crucial role in the human body. It could produce anti-tumor tin compounds in the human thymus gland. Furthermore, it also could promote the synthesis of proteins and nucleic acids and affect the function of hemoglobin, etc. Sn^{4+} have been found to coordinate with many natural products for use in the treatment of tumors. Ferulic acid (FA) is a polyphenolic component from natural plants with antioxidant and anti-tumor effects. Pellerito et al. synthesized a new complex (ferulate (TBT-F) by coordinating tributyltin (IV) with FA. Sn^{4+} was at least penta-coordinated and the ligand acted as a monoanionic ligand by bridging the carboxylate anion. TBT-F possessed a significant killing effect on HCT116, HT-29 and Caco-2 colon cancer cells in a concentration range of nM, whereas FA without Sn coordination was ineffective under the same conditions [160]. Natural bacteriochlorophyll A was coordinated with Sn to form a complex with a photodynamic property to exert PDT for treating tumors [161]. Representative natural products coordinated with Sn^{4+}were displayed in Table 6.

Table 5 Representative natural products coordinated with Zn^{2+}

NO	Natural products	Metal ions	Preparation	TME Response	Size	Treatment	Bioimaging	Reference
1	Fluorouracil	Zn^{2+}	Ultrasound	pH/ATP	100 nm	ICD	FI	[150]
2	IR780-1, 2-methyl-imidazole, siRNA	Zn^{2+}	Stirring	NIR	150–200 nm	PTT/GT	PTI/PAI/FI	[156]
3	RNA	Zn^{2+}	Stirring	–	60–120 nm	CT	FI	[151]
4	L-cystine	Zn^{2+}	Stirring	GSH	189.1 ± 3.8 nm	CT	–	[152]
5	Dipicolylamine-Arg-Gly-Asp, Au, ICG	Zn^{2+}	In Vivo assembled	NIR	100 nm	PTT	FI/PAI/MRI	[153]

Table 6 Representative natural products coordinated with Co^{3+}, $Mo^{4+/5+}$, Sn^{4+}, Ni^{2+}, $V^{3+/4+/5+}$ and multiple ions

NO	Natural Products	Metal ions	Preparation	TME Response	Size	Treatment	Bioimaging	Reference
1	Tetrakis(4-carboxyphenyl) porphyrin, TCPP; triphenylphosphonium,TPP	Co^{3+}	ultrasound	US	962.2 ± 8.739 nm, 2 nm	SDT	FI	[157]
2	Epigallocatechin gallate, EGCG	Mo^{5+}	biomineralization	GSH	4.75 ± 0.06 nm	CDT/ICD	–	[158]
3	Polyethylene glycol, PEG	Mo^{4+}	hydrothermal method; Stirring	–	~400 nm	CT	–	[172]
4	Polydopamine, PDA	Mo^{4+}	Stirring	pH/ NIR	50–100 nm	CT/PTT	FI/PAI/MRI	[159]
5	Ferulic acid	Sn^{4+}	–	–	–	CT	–	[160]
6	Natural bacteriochlorophyll A	Sn^{4+}	Stirring	NIR	–	PDT/CT	–	[161]
7	Schiff base	Ni^{2+}	–	–	–	CT	–	[173]
8	Tannic acid, TA	V^{5+}	Magnetic stirring	pH	130 nm	PTT/CDT	PTI	[167]
9	Tannic acid, TA	V^{4+}	Magnetic stirring	–	80 nm	PTT/ICD	–	[168]
10	Tris-catechol	V^{3+}	Magnetic stirring	pH	231 nm	CT	–	[174]
11	Tannic acid, TA	V^{5+}	Magnetic stirring	pH	71.8 nm	ICD/CDT	FI	[175]
12	Tannic acid, TA	Fe^{3+}/ Mn^{2+}	Magnetic stirring	NIR	168 nm	ICD/PTT/CDT	PTI	[169]
13	Linoleic acid hydroperoxide, LAHP	Cu^{2+}/ Fe^{3+}	Magnetic stirring	pH	~100 nm	PDT/ICD	–	[104]
14	Gossypol	Co^{3+}/ Fe^{3+}	Ultrasound	NIR	60 nm	CT/PTT	FI/MRI	[58]

Natural product-coordinated Ni^{2+} self-assembly

In our daily diet, chocolate, nuts and cereals are rich in nickel, which are one of the essential trace elements and possess the ability to stimulate hematopoiesis. Hosseini et al. prepared a series of nickel SCS complexes characterized by a stable mesophenylene center and two unstable thioamides donors at the periphery of the ligand. The results demonstrated its effect on the treatment of estrogen-dependent mammary tumor cells (MCF-7 and MC4L2) and proliferation of triple-negative breast cancer (4T1) [162]. Pham et al. prepared six new nickel-Schiff base complexes with potential as lead complexes for DNA binding studies and also showed the ability to induce apoptosis in cancer cells [163]. Representative natural products coordinated with Ni^{2+} were displayed in Table 6.

Natural product-coordinated $V^{3+/4+/5+}$ self-assembly

Vanadium is one of the essential trace elements for the human body. As researched, it is extremely closely related to the human body's nervous, hematopoietic, cardiovascular systems and cholesterol metabolism, as well as the kidneys, liver and bones, affecting human health. Among the potential pharmacological effects of Vanadium compounds, its hypoglycemic and anticancer effects are the most noticeable. However, the toxicity of Vanadium should not be overlooked [163–165]. Several studies have been conducted to employ V-coordinated nanomedicines for in vivo tumor-selective therapy and imaging [166]. In a study, a simple one-step assembly method was utilized to successfully prepare a novel natural polyphenolic TA coordinated mixed-valence V oxide nanoparticles. V valence shift catalyzed the production of toxic ·OH from H_2O_2 to achieve tumor-specific CDT. In addition, NIR absorption enabled tumor PTT. In vitro and in vivo experiments showed that the synergistic strategy of CDT and PTT effectively inhibited tumor growth [167]. Hu et al. designed a V-based nanocomplex that coordinated vanadyl ions (VO^{2+}) with TA and integrated filaggrin proteins (SS) through complex interactions. V-based nanocomplexes exerted a PTT effect that ablated in situ tumors and triggered ICD via endoplasmic reticulum stress to activate systemic immune responses for better suppression of distal tumors [168]. Zhang et al. proposed a mode of enhanced ferroptosis activation through modulation of tumor cell glucose metabolism by utilizing TA coordinated with V oxides and loaded with lonidamine (LND). Valence changes of V induced ferroptosis, while LND enhanced ferroptosis-induced immune activation by interfering with glucose metabolism. This synergistic treatment provides a new option for tumor therapy [80]. Representative natural products coordinated with $V^{3+/4+/5+}$ were displayed in Table 6.

Natural product-coordinated multiple metal self-assembly

Combined coordination of multiple metals is an effective synergy strategy for treating tumors. TA coordinated with Fe^{3+}/Mn^{2+} loading with PD-L1 inhibiting DNAzyme to form an all-active component nanoplatform named MPNS. The valence transition of Fe^{3+} after entering tumor cells triggered ferroptosis, whereas DNAzyme activated by Mn^{2+} effectively silenced PD-L1. In the meantime, ferroptosis could activate the immune response by triggering ICD. Ferroptosis induced immunotherapy was applicable to the treatment of primary and distant tumors [169]. Additionally, amino acids were linked to DOX through click chemistry for the purpose of targeted drug release in the TME and MRI-mediated tumor therapy through the action of amino-coordination metal ions (Gd^{3+}, Fe^{3+}, and Mn^{2+}) [170]. Singh et al. coordinated Zn^{2+} with CuO by sonochemistry and then modified the surface of the nanoparticles with folic acid-modified alginate coupled with polydopamine for targeted delivery of PTX for the treatment of breast cancer. It also further induced cell death by increasing intracellular ROS production for synergistic treatment of tumors with PTX chemotherapy and oxidative stress. To test the ability of NPs to generate ROS, the results detected with the DCFH-DA probe demonstrated that Zn^{2+} doping in the CuO skeleton significantly increased the PTX loading rate, and NPs-treated MCF-7 cells produced more ROS than free PTX [171].

Zeng et al. coordinated $CoFe_2O_4$ with gossypol and encapsulated it with glycerol monooleate (GMO) to form NPs. To verify the targeting properties of NPs, the investigators labeled NPs with IR780, which showed satisfactory tumor-targeting properties by in vivo fluorescence after injection into mice. In addition, they demonstrated by fluorescence imaging of isolated organs that the synthesized nanoparticles had better tumor site aggregation and longer tumor retention time compared to free IR780 [58]. Zhang et al. synthesized an ultra-small nanoparticle by the BCGN@L with Bi/Cu-GA coordination and then loaded polyvinylpyrrolidone and glucose oxidase (Gox). Upon arrival at the tumor site, GOx catalyzed glucose to produce gluconic acid and H_2O_2 for CDT. Glucose depletion reduced the expression of heat shock proteins (HSPs) and enhanced the sensitivity of PTT, resulting in a synergistic effect of CDT and PTT [123]. Liu et al. coordinated TA with Fe^{3+}/Mn^{2+} and encapsulated it with Anti PD-L1 DNAzyme to form a fully active component nanoplatform. The valence state transition of Fe3 + entering tumor cells triggers ferroptosis, while Mn2 + activated DNAzyme effectively silences PD-L1. Meanwhile, ferroptosis can activate immune responses by triggering ICD, which is suitable for the treatment of primary and distant tumors (Fig. 8) [169]. Representative natural products coordinated with multiple ions were displayed in Table 6.

Biological safety

Few studies have reported significant biotoxicity of metal ions when coordinated with natural products. Numerous studies have confirmed the good biodegradability and biocompatibility of the coordination with metal ions [102, 144, 156, 176]. Although a variety of metal-coordinated nanoparticles have been demonstrated to exert significant antitumor activity, there are still no clear standard to assess the biosafety of metal nanoparticles. Undoubtedly, the content of metal ions directly affects their toxicity. For example, iron overload causes biotoxicity, and the poor prognosis of many diseases is associated with it. In patients with severe iron loading, iron could cause severe organ damage and death [177]. Excessive intake of zinc ions could cause nausea, diarrhea and abdominal discomfort. In severe cases, it could adversely affect the lipid profile of the body and the immune system [178]. The daily intake of some trace elements copper, iron, manganese, molybdenum, selenium, and zinc is as follows: 0.3–0.5 mg, 1 mg, 55 μg, 19–25 μg, 60–100 μg, and 3–5 mg [179].

In addition, the toxicity of metal-coordinated nanoparticles depends on their biophysical properties such as size, specific surface area, surface charge and aggregation state [180]. Therefore, it is crucial to establish a standard for evaluating the safety of metal ions coordination.

Conclusion and perspective

The review summarizes the research advances in nanomedicines formed by natural products coordinated with metal ions for multimodal imaging and multi-modality combination therapy of tumors in the last 3–4 years. The metal ions listed are all essential metal elements in human body, these natural products are derived from various plant and animal extracts, natural ingredient derivatives, and microbial metabolites, which are combined with metal ions to create more unexpected effects from the original active ingredients. These nanomedicines are being extensively studied for treatment of tumors.

First of all, Sources of material for natural products are widespread. They are critical material to cure various diseases and mainly derived from various plants, animals, microorganisms and some natural product derivatives. Such as tannic acid, curcumin and other polyphenols extracted from a variety of plants. DOX extracted from the fermentation broth of Streptomyces bosaiensis var. sp. They have been widely investigated in nano-delivery field because their structural characteristics make them easy to coordinated assembly. These natural products

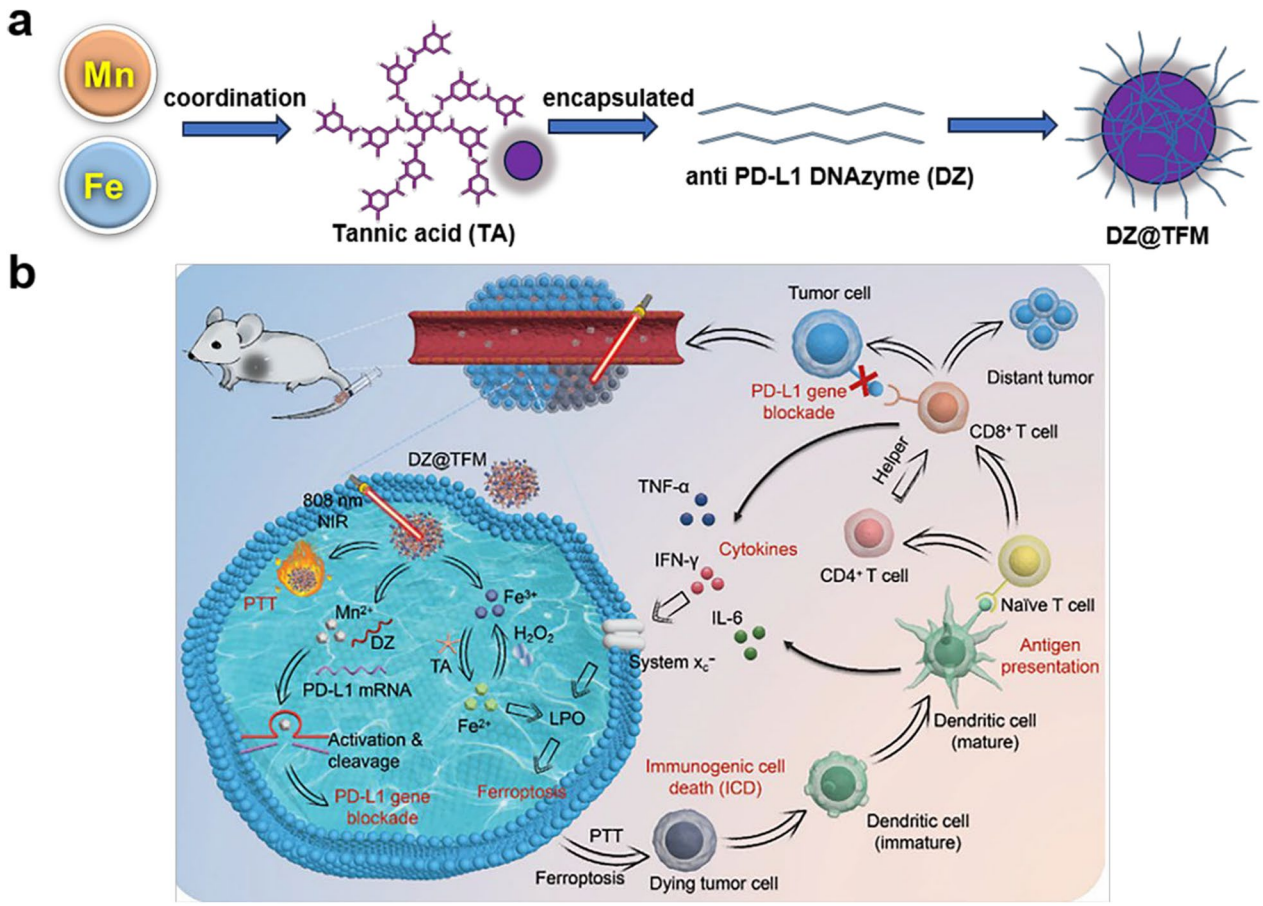

Fig. 8 Schematic representation of a nanoplatform of TA coordinated with Fe^{3+}/Mn^{2+} and encapsulated with Anti PD-L1 DNAzyme to form a fully active component and the combination of multiple therapeutics. Copyright 2022, Wiley

possess various biological activities, and most of them are natural small molecules with high safety and unexpected development and utilization value.

Secondly, the coordinated self-assembled nanomedicine synthesis is green and simple. Natural products and metal ions are generally synthesized by simple ways such as stirring, ultrasonic, redox, and one-pot method due to the coordination effect as well as π-π stacking effect. The preparation processed simple, environmentally friendly and time-saving. Moreover, the particle size and other characteristics of nanoparticles can be controlled by adjusting the ratio of raw materials and the synthesis time, which is more convenient than the preparation of other new nanomaterials.

Thirdly, multiple imaging modalities and combined treatment of multiple modalities for tumors are hot topics in current research. Drug pathways as well as treatment effects are monitored through in vivo imaging. Obviously, combination therapy is promised to serve as an effective measure to ameliorate drug resistance in tumor cells. New functions emerged on the basis of the original efficacy due to the successful coordination of metal ions with natural products. The propensity of metal ions to coordinate with natural products is determined by a variety of chemical properties, including the charge density, electronic structure, and coordination geometry preference of the metal ion, as well as the electron-giving capacity and spatial configuration of the ligand in the natural product. Metal ions with higher electron cloud densities tend to coordinate with organic molecules containing more π-electrons or lone pairs of electrons, while metal ions with lower electron cloud densities tend to coordinate with molecules containing electronegative atoms such as oxygen and nitrogen. In natural products, functional groups (e.g., hydroxyl, amino, carbonyl, etc.) containing atoms such as oxygen and nitrogen are usually used as coordination sites. Metal ions such as $Fe^{2+/3+}$, $Cu^{+/2+}$, Zn^{2+}, Ni^{2+} and other transition metal ions are often able to form stable coordination compounds with multiple coordination sites in natural products due to their variable oxidation states and strong field strengths. For example, $Fe^{2+/3+}$ and $Cu^{+/2+}$ are easy to change their

valence states due to tumor environmental influences. Therefore, the nanomedicine coordinated with them exert CDT through amplify oxidative stress. The coordination of some metal ions (such as Mn^{2+}/Cu^{2+}/$Fe^{2+/3+}$) with natural products also shows photoacoustic signals, they are utilized to accurately measure and quantify vascular morphology, blood flow, monitor tumor oxygen/hypoxia status and the depth of drug reaching the tumor, etc. Even the diagnosis and surgery of complex diseases are guided by precise imaging. In addition, natural products can also be used in other therapeutic methods such as chemotherapy and immunotherapy due to their combination with metal ions, and have various imaging functions, such as enhanced magnetic resonance imaging of divalent manganese ions (Mn^{2+}) and fluorescence imaging of rare earth metal ion complexes. In summary, if researchers want to develop nanomedicines for oxidative stress, they can preferably choose metal ions with easily changeable valence states such as $Fe^{2+/3+}$, $Cu^{+/2+}$, $V^{3+/4+/5+}$ to assemble with suitable natural products in coordination, which will endow them with excellent photo-thermal effects and amplified oxidative stress. If immune activation is required, $Mn^{2+/3+}$ and Zn^{2+} can be selected for coordination with suitable natural products to activate the body's own powerful immune response for primary as well as distant tumour treatment. In terms of imaging, Mn^{2+} is widely used in nuclear magnetic imaging. In addition, photoacoustic imaging can also be achieved through metal ions such as $Fe^{2+/3+}$, $Cu^{+/2+}$, $Mn^{2+/3+}$, etc.

In conclusion, this review lists a large number of studies describing the combination of multiple imaging modalities of PTI/FLI/PAI/MRI with CT/CDT/PTT/PDT/ICD/SDT for the treatment of tumors. It is proved that natural products coordinated with metal ions possess broad application prospects in treating tumors, fighting tumor drug resistance, and detecting and treating more complex tumors. However, there are still challenges in certain key technical routes and practical applications. The first is the safety issue, excessive metal ions will produce toxicity, so it is necessary to determine the ratio of raw materials and methods, and at the same time to keep the nanomedicine in the physiological state of stability, cannot be released prematurely to cause damage to the organism. Next is the stability problem, the formation of aggregated precipitates will make the particle size increase thus affecting the penetration rate. If the above problems can be solved, the nanomedicines have stable performance and can be released precisely. It is believed that the natural product-coordinated metal nanomedicines for multi-modality imaging-mediated multi-pathway tumor therapy strategy have a broad application prospect, and will be one of the indispensable pathways for future tumor therapy.

Acknowledgements
This work was supported by the National Natural Science Foundation of China (82104357), China Postdoctoral Science Foundation (2022T150441 and 2021M702292).

Author contributions
L.XY. and L.SY. collected resources and wrote the main manuscript text and design pictures; J.XY., L.HF. and W.XQ. participated in resource collecting of the article; S.KH., L.MF., W.P. and C.YX. participated in text proofreading of the article; W.TJ. and W.B. participated in the overall idea design and supervision of the article; Y.XA. designed, supervised, revised and edited the main manuscript. All authors reviewed the manuscript, all authors have approved the submitted version and have agreed both to be personally accountable for the author's own contributions.

Funding
National Natural Science Foundation of China (82104357); China Postdoctoral Science Foundation (2022T150441 and 2021M702292).

Availability of data and materials
No datasets were generated or analyzed during the current study.

Declarations

Ethics approval and consent to participate
Not applicable.

Consent for publication
All authors have read the journal policies and submit this manuscript in accordance with those policies. All authors agree to publish.

Competing interests
The authors declare that they have no competing interests.

Author details
[1]School of Pharmacy, Shenyang Pharmaceutical University, Shenyang 110016, China. [2]State Key Laboratory of Component-Based Chinese Medicine, Tianjin University of Traditional Chinese Medicine, Tianjin 301617, China. [3]NMPA Key Laboratory for Bioequivalence Research of Generic Drug Evaluation, Shenzhen Institute for Drug Control, Shenzhen 518057, China. [4]NMPA Key Laboratory for Quality Research and Evaluation of Traditional Chinese Medicine, Shenzhen Institute for Drug Control, Shenzhen 518057, China.

Received: 31 May 2024 Accepted: 4 November 2024
Published online: 21 November 2024

References

1. Heneberg P. Lactic acidosis in patients with solid cancer. Antioxid Redox Signal. 2022;37:1130–52.
2. Ratanasrimetha P, Workeneh BT, Seethapathy H. Sodium and potassium dysregulation in the patient with cancer. Adv Chronic Kidney Dis. 2022;29:171-179.e1.
3. Sun J, Luo C, Wang Y, He Z. The holistic 3M modality of drug delivery nanosystems for cancer therapy. Nanoscale. 2013;5:845–59.
4. Chen S, Fan JX, Zheng DW, Liu F, Zeng X, Yan GP, Zhang XZ. A multi-functional drug delivery system based on polyphenols for efficient tumor inhibition and metastasis prevention. Biomater Sci. 2020;8:702–11.
5. Hwang E, Jung HS. Metal-organic complex-based chemodynamic therapy agents for cancer therapy. Chem Commun. 2020;56:8332–41.
6. Qin J, Guo N, Yang J, Chen Y. Recent advances of metal-polyphenol coordination polymers for biomedical applications. Biosensors. 2023;13:776.
7. Naeem A, Hu P, Yang M, Zhang J, Liu Y, Zhu W, Zheng Q. Natural products as anticancer agents: current status and future perspectives. Molecules. 2022;27:8367.

8. Liu Y, Yang S, Wang K, Lu J, Bao X, Wang R, Qiu Y, Wang T, Yu H. Cellular senescence and cancer: focusing on traditional Chinese medicine and natural products. Cell Prolif. 2020;53: e12894.
9. Gupta D, Boora A, Thakur A, Gupta TK. Green and sustainable synthesis of nanomaterials: recent advancements and limitations. Environ Res. 2023;231: 116316.
10. Wang Z, Yang L. Natural-product-based, carrier-free, noncovalent nanoparticles for tumor chemo-photodynamic combination therapy. Pharmacol Res. 2024;203: 107150.
11. Zhang W, Li S, Li C, Li T, Huang Y. Remodeling tumor microenvironment with natural products to overcome drug resistance. Front Immunol. 2022;13:1051998.
12. Rajabi S, Maresca M, Yumashev AV, Choopani R, Hajimehdipoor H. The most competent plant-derived natural products for targeting apoptosis in cancer therapy. Biomolecules. 2021;11:534.
13. Liu Y, Wang Y, Song S, Zhang H. Cancer therapeutic strategies based on metal ions. Chem Sci. 2021;12:12234–47.
14. Hopff SM, Wang Q, Frias C, Ahrweiler M, Wilke N, Wilke N, Berkessel A, Prokop A. A metal-free salalen ligand with anti-tumor and synergistic activity in resistant leukemia and solid tumor cells via mitochondrial pathway. J Cancer Res Clin Oncol. 2021;147:2591–607.
15. Liang S, Wang M, Wang J, Chen G. Red-blood-cell-membrane-coated metal-drug nanoparticles for enhanced chemotherapy. ChemBioChem. 2021;22:3184–9.
16. Lan Z, Tan X, Chen C, Cao Y, Wan Y, Feng S. Folate-mediated magnetic and pH/GSH dual-responsive metal-polymer-coordinated nanocomplexes for joint chemo/chemodynamic anti-breast cancer therapy. J Biomater Sci Polym Ed. 2023;34:2041–59.
17. Pan MM, Li P, Yu YP, Jiang M, Yang X, Zhang P, Nie J, Hu J, Yu X, Xu L. Bimetallic ions functionalized metal-organic-framework nanozyme for tumor microenvironment regulating and enhanced photodynamic therapy for hypoxic tumor. Adv Healthc Mater. 2023;12: e2300821.
18. Liu B, Jiao J, Xu W, Zhang M, Cui P, Guo Z, Deng Y, Chen H, Sun W. Highly efficient far-red/NIR-absorbing neutral Ir(III) complex micelles for potent photodynamic/photothermal therapy. Adv Mater. 2021;33: e2100795.
19. Wu Y, Song X, Xu W, Sun KY, Wang Z, Lv Z, Wang Y, Wang Y, Zhong W, Wei J, et al. NIR-activated multimodal photothermal/chemodynamic/magnetic resonance imaging nanoplatform for anticancer therapy by Fe(II) ions doped MXenes (Fe-Ti(3) C(2)). Small. 2021;17: e2101705.
20. Kang Y, Zhai X, Lu S, Vuletic I, Wang L, Zhou K, Peng Z, Ren Q, Xie Z. A hybrid imaging platform(CT/PET/FMI) for evaluating tumor necrosis and apoptosis in real-time. Front Oncol. 2022;12: 772392.
21. Li L, Ding W, Huang L, Zhuang X, Grau V. Multi-modality cardiac image computing: A survey. Med Image Anal. 2023;88: 102869.
22. Li Y, Pan X, Hai P, Zheng Y, Shan Y, Zhang J. All-in-one nanotheranostic platform based on tumor microenvironment: new strategies in multimodal imaging and therapeutic protocol. Drug Discov Today. 2024;29: 104029.
23. Gu M, Zhang L, Hao L, Wang K, Yang W, Liu Z, Lei Z, Zhang Y, Li W, Jiang L, et al. Upconversion nanoplatform enables multimodal imaging and combinatorial immunotherapy for synergistic tumor treatment and monitoring. ACS Appl Mater Interfaces. 2023;15:21766–80.
24. Li P, Wang D, Hu J, Yang X. The role of imaging in targeted delivery of nanomedicine for cancer therapy. Adv Drug Deliv Rev. 2022;189: 114447.
25. Xu J, Wang J, Ye J, Jiao J, Liu Z, Zhao C, Li B, Fu Y. Metal-Coordinated Supramolecular Self-Assemblies for Cancer Theranostics. Adv Sci. 2021;8: e2101101.
26. Xie L, Li J, Wang L, Dai Y. Engineering metal-phenolic networks for enhancing cancer therapy by tumor microenvironment modulation. Wiley Interdiscip Rev Nanomed Nanobiotechnol. 2023;15: e1864.
27. Zheng S, Wang X, Zhao D, Liu H, Hu Y. Calcium homeostasis and cancer: insights from endoplasmic reticulum-centered organelle communications. Trends Cell Biol. 2023;33:312–23.
28. Yang Y, Wang P, Cheng H, Cheng Y, Zhao Z, Xu Y, Shen Y, Zhu M. A multi-responsive Au NCs@PMLE/Ca(2+) antitumor hydrogel formed in situ on the interior/surface of tumors for PT imaging-guided synergistic PTT/O(2)-enhanced PDT effects. Nanoscale. 2022;14:7372–86.
29. Sharma A, Kumar A, Li C, Panwar Hazari P, Mahajan SD, Aalinkeel R, Sharma RK, Swihart MTA. cannabidiol-loaded Mg-gallate metal-organic framework-based potential therapeutic for glioblastomas. J Mater Chem B. 2021;9:2505–14.
30. Jing W, Xiaolan C, Yu C, Feng Q, Haifeng Y. Pharmacological effects and mechanisms of tannic acid. Biomed Pharmacother. 2022;154: 113561.
31. Shim G, Ko S, Park JY, Suh JH, Le QV, Kim D, Kim YB, Im GH, Kim HN, Choe YS, et al. Tannic acid-functionalized boron nitride nanosheets for theranostics. J Control Release. 2020;327:616–26.
32. Luo Y, Qiao B, Zhang P, Yang C, Cao J, Yuan X, Ran H, Wang Z, Hao L, Cao Y, et al. TME-activatable theranostic nanoplatform with ATP burning capability for tumor sensitization and synergistic therapy. Theranostics. 2020;10:6987–7001.
33. Li J, Li X, Gong S, Zhang C, Qian C, Qiao H, Sun M. Dual-mode avocado-like all-iron nanoplatform for enhanced T(1)/T(2) MRI-guided cancer theranostic therapy. Nano Lett. 2020;20:4842–9.
34. Huang X, Tian X, Zhang Q, Hu H, Gao J, Ma B, Wu K, Bai J, Du S, Lu Y, et al. Combined photothermal-immunotherapy via poly-tannic acid coated PLGA nanoparticles for cancer treatment. Biomater Sci. 2021;9:6282–94.
35. Tian F, Wang S, Shi K, Zhong X, Gu Y, Fan Y, Zhang Y, Yang M. Dual-depletion of intratumoral lactate and ATP with radicals generation for cascade metabolic-chemodynamic therapy. Adv Sci. 2021;8: e2102595.
36. Zhang C, Li J, Yang C, Gong S, Jiang H, Sun M, Qian C. A pH-sensitive coordination polymer network-based nanoplatform for magnetic resonance imaging-guided cancer chemo-photothermal synergistic therapy. Nanomedicine. 2020;23: 102071.
37. Liu C, Li C, Jiang S, Zhang C, Tian Y. pH-responsive hollow Fe-gallic acid coordination polymer for multimodal synergistic-therapy and MRI of cancer. Nanoscale Adv. 2021;4:173–81.
38. Tian Q, Cai Y, Li N, Liu Q, Gu B, Chen ZG, Song S. Ellagic acid-Fe nanoscale coordination polymer with higher longitudinal relaxivity for dual-modality T(1)-weighted magnetic resonance and photoacoustic tumor imaging. Nanomedicine. 2020;28: 102219.
39. Chen G, Yang Y, Xu Q, Ling M, Lin H, Ma W, Sun R, Xu Y, Liu X, Li N, et al. Self-amplification of tumor oxidative stress with degradable metallic complexes for synergistic cascade tumor therapy. Nano Lett. 2020;20:8141–50.
40. Zhang X, Si Z, Wang Y, Li Y, Xu C, Tian H. Polymerization and coordination synergistically constructed photothermal agents for macrophages-mediated tumor targeting diagnosis and therapy. Biomaterials. 2021;264: 120382.
41. Wang B, Dai Y, Kong Y, Du W, Ni H, Zhao H, Sun Z, Shen Q, Li M, Fan Q. Tumor microenvironment-responsive Fe(III)-porphyrin nanotheranostics for tumor imaging and targeted chemodynamic-photodynamic therapy. ACS Appl Mater Interfaces. 2020;12:53634–45.
42. Xu H, Yu N, Zhang J, Wang Z, Geng P, Wen M, Li M, Zhang H, Chen Z. Biocompatible Fe-hematoporphyrin coordination nanoplatforms with efficient sonodynamic-chemo effects on deep-seated tumors. Biomaterials. 2020;257: 120239.
43. Fan Z, Shi D, Zuo W, Feng J, Ge D, Su G, Yang L, Hou Z. Trojan-horse diameter-reducible nanotheranostics for macroscopic/microscopic imaging-monitored chemo-antiangiogenic therapy. ACS Appl Mater Interfaces. 2022;14:5033–52.
44. Chen J, Wang X, Zhang Y, Zhang S, Liu H, Zhang J, Feng H, Li B, Wu X, Gao Y, et al. A redox-triggered C-centered free radicals nanogenerator for self-enhanced magnetic resonance imaging and chemodynamic therapy. Biomaterials. 2021;266: 120457.
45. Li Z, Wu X, Wang W, Gai C, Zhang W, Li W, Ding D. Fe(II) and tannic acid-cloaked mof as carrier of artemisinin for supply of ferrous ions to enhance treatment of triple-negative breast cancer. Nanoscale Res Lett. 2021;16:37.
46. Mu M, Chen H, Fan R, Wang Y, Tang X, Mei L, Zhao N, Zou B, Tong A, Xu J, et al. A tumor-specific ferric-coordinated epigallocatechin-3-gallate cascade nanoreactor for glioblastoma therapy. J Adv Res. 2021;34:29–41.
47. Feng W, Shi W, Liu S, Liu H, Liu Y, Ge P, Zhang H. Fe(III)-Shikonin supramolecular nanomedicine for combined therapy of tumor via ferroptosis and necroptosis. Adv Healthc Mater. 2022;11: e2101926.
48. Feng W, Shi W, Wang Z, Cui Y, Shao X, Liu S, Rong L, Liu Y, Zhang H. Enhancing tumor therapy of Fe(III)-shikonin supramolecular nanomedicine via triple ferroptosis amplification. ACS Appl Mater Interfaces. 2022;14:37540–52.
49. Yu X, Han N, Dong Z, Dang Y, Zhang Q, Hu W, Wang C, Du S, Lu Y. Combined chemo-immuno-photothermal therapy for effective cancer

treatment via an all-in-one and one-for-all nanoplatform. ACS Appl Mater Interfaces. 2022;14:42988–3009.
50. Meng J, Xin L, Zou B, Wang L, Zhao X, Gao J, Zhang R. A manual controlled theranostic nanoplatform with real-time photoacoustic quantification of drug release for chemophotothermal therapy. J Colloid Interface Sci. 2023;651:1020–7.
51. Nie T, Liu H, Fang Z, Zheng Y, Zhang R, Xu X, Liu S, Wu J. Tumor microenvironment mediated spermidine-metal-immunopeptide nanocomplex for boosting ferroptotic immunotherapy of lymphoma. ACS Nano. 2023;17:10925–37.
52. Shi H, Xiong CF, Zhang LJ, Cao HC, Wang R, Pan P, Guo HY, Liu T. Light-triggered nitric oxide nanogenerator with high l-arginine loading for synergistic photodynamic/gas/photothermal therapy. Adv Healthc Mater. 2023;12: e2300012.
53. Li J, Song J, Deng Z, Yang J, Wang X, Gao B, Zhu Y, Yang M, Long D, Luo X, et al. Robust reactive oxygen species modulator hitchhiking yeast microcapsules for colitis alleviation by trilogically intestinal microenvironment renovation. Bioact Mater. 2024;36:203–20.
54. Deng Z, Ma W, Ding C, Wei C, Gao B, Zhu Y, Zhang Y, Wu F, Zhang M, Li R, et al. Metal polyphenol network/cerium oxide artificial enzymes therapeutic nanoplatform for MRI/CT-aided intestinal inflammation management. Nano Today. 2023;53: 102044.
55. Zeng F, Tang L, Zhang Q, Shi C, Huang Z, Nijiati S, Chen X, Zhou Z. Coordinating the mechanisms of action of ferroptosis and the photothermal effect for cancer theranostics. Angew Chem Int Ed Engl. 2022;61: e202112925.
56. Guan J, Tan X, Jiao J, Lai S, Zhang H, Kan Q, He Z, Sun M, Sun J. Iron ion-coordinated carrier-free supramolecular co-nanoassemblies of dual DNA topoisomerase-targeting inhibitors for tumor suppression. Acta Biomater. 2022;144:121–31.
57. Zhang Z, Pan Y, Cun JE, Li J, Guo Z, Pan Q, Gao W, Pu Y, Luo K, He B. A reactive oxygen species-replenishing coordination polymer nanomedicine disrupts redox homeostasis and induces concurrent apoptosis-ferroptosis for combinational cancer therapy. Acta Biomater. 2022;151:480–90.
58. Zeng Y, Liu H, Ma J, Li K, Chang P, Wang C, Li L, Chen D, Liu C, Li N, et al. Cobalt ferrite-gossypol coordination nanoagents with high photothermal conversion efficiency sensitizing chemotherapy against Bcl-2 to induce tumor apoptosis. Small. 2023;19: e2300104.
59. Huang S, Le H, Hong G, Chen G, Zhang F, Lu L, Zhang X, Qiu Y, Wang Z, Zhang Q, et al. An all-in-one biomimetic iron-small interfering RNA nanoplatform induces ferroptosis for cancer therapy. Acta Biomater. 2022;148:244–57.
60. Guo X, Cai Q, Lian X, Fan S, Hu W, Cui W, Zhao X, Wu Y, Wang H, Wu Y, et al. Novel Fe(III)-polybasic acid coordination polymer nanoparticles with targeted retention for photothermal and chemodynamic therapy of tumor. Eur J Pharm Biopharm. 2021;165:174–84.
61. Zhou H, He G, Sun Y, Wang J, Wu H, Jin P, Zha Z. Cryptobiosis-inspired assembly of "AND" logic gate platform for potential tumor-specific drug delivery. Acta Pharm Sin B. 2021;11:534–43.
62. Liu Z, Hu C, Liu S, Cai L, Zhou Y, Pang M. Facile synthesis of Fe-baicalein nanoparticles for photothermal/chemodynamic therapy with accelerated Fe(III)/Fe(II) conversion. J Mater Chem B. 2021;9:3295–9.
63. Yang B, Yao H, Tian H, Yu Z, Guo Y, Wang Y, Yang J, Chen C, Shi J. Intratumoral synthesis of nano-metalchelate for tumor catalytic therapy by ligand field-enhanced coordination. Nat Commun. 2021;12:3393.
64. Han Y, Dong Z, Wang C, Li Q, Hao Y, Yang Z, Zhu W, Zhang Y, Liu Z, Feng L. Ferrous ions doped calcium carbonate nanoparticles potentiate chemotherapy by inducing ferroptosis. J Control Release. 2022;348:346–56.
65. He X, Zhu H, Shang J, Li M, Zhang Y, Zhou S, Gong G, He Y, Blocki A, Guo J. Intratumoral synthesis of transformable metal-phenolic nanoaggregates with enhanced tumor penetration and retention for photothermal immunotherapy. Theranostics. 2022;12:6258–72.
66. Liu H, Zhang M, Jin H, Tao K, Tang C, Fan Y, Liu S, Liu Y, Hou Y, Zhang H. Fe(III)-doped polyaminopyrrole nanoparticle for imaging-guided photothermal therapy of bladder cancer. ACS Biomater Sci Eng. 2022;8:502–11.
67. Wang Y, Chen J, Lu J, Xi J, Xu Z, Fan L, Dai H, Gao L. Metal ions/nucleotide coordinated nanoparticles comprehensively suppress tumor by synergizing ferroptosis with energy metabolism interference. J Nanobiotechnol. 2022;20:199.
68. Xu Y, Guo Y, Zhang C, Zhan M, Jia L, Song S, Jiang C, Shen M, Shi X. Fibronectin-coated metal-phenolic networks for cooperative tumor chemo-/chemodynamic/immune therapy via enhanced ferroptosis-mediated immunogenic cell death. ACS Nano. 2022;16:984–96.
69. Yu H, Li Y, Zhang Z, Ren J, Zhang L, Xu Z, Kang Y, Xue P. Silk fibroin-capped metal-organic framework for tumor-specific redox dyshomeostasis treatment synergized by deoxygenation-driven chemotherapy. Acta Biomater. 2022;138:545–60.
70. Zhang J, Sun X, Zhao X, Yang C, Shi M, Zhang B, Hu H, Qiao M, Chen D, Zhao X. Combining immune checkpoint blockade with ATP-based immunogenic cell death amplifier for cancer chemo-immunotherapy. Acta Pharm Sin B. 2022;12:3694–709.
71. Zhao F, Qian Y, Li H, Yang Y, Wang J, Yu W, Li M, Cheng W, Shan L. Amentoflavone-loaded nanoparticles enhanced chemotherapy efficacy by inhibition of AKR1B10. Nanotechnology. 2022;33: 385101.
72. Zhu C, Wang Y, Li Z, Sun W, Jiang BP, Shen XC. Metallopolysaccharide-based smart nanotheranostic for imaging-guided precise phototherapy and sequential enzyme-activated ferroptosis. Biomacromol. 2022;23:2007–18.
73. Chen J, Zhang J, Wei X, Zhang Y, Hu J, Liu H, Zhang S, Yang B. Chemodynamic therapy agent optimized mesoporous TiO(2) nanoparticles for glutathione-enhanced and hypoxia-tolerant synergistic chemosonodynamic therapy. J Colloid Interface Sci. 2023;650:1773–85.
74. Liu S, Zhang M, Jin H, Wang Z, Liu Y, Zhang S, Zhang H. Iron-containing protein-mimic supramolecular iron delivery systems for ferroptosis tumor therapy. J Am Chem Soc. 2023;145:160–70.
75. Shi H, Wang R, Cao HC, Guo HY, Pan P, Xiong CF, Zhang LJ, Yang Q, Wei S, Liu T. A metal-polyphenol-based oxygen economizer and fenton reaction amplifier for self-enhanced synergistic photothermal/chemodynamic/chemotherapy. Adv Healthc Mater. 2023;12: e2300054.
76. Wang S, Guo Q, Xu R, Lin P, Deng G, Xia X. Combination of ferroptosis and pyroptosis dual induction by triptolide nano-MOFs for immunotherapy of melanoma. J Nanobiotechnol. 2023;21:383.
77. Wang TH, Shen MY, Yeh NT, Chen YH, Hsu TC, Chin HY, Wu YT, Tzang BS, Chiang WH. Photothermal nanozymes to self-augment combination cancer therapy by dual-glutathione depletion and hyperthermia/acidity-activated hydroxyl radical generation. J Colloid Interface Sci. 2023;650:1698–714.
78. Yu J, Zhang Y, Li L, Xiang Y, Yao X, Zhao Y, Cai K, Li M, Li Z, Luo Z. Coordination-driven FBXW7 DNAzyme-Fe nanoassembly enables a binary switch of breast cancer cell cycle checkpoint responses for enhanced ferroptosis-radiotherapy. Acta Biomater. 2023;169:434–50.
79. Zhang D, Jiang C, Zheng X, Lin Z, Zhuang Q, Xie H, Liang Y, Xu Y, Cui L, Liu X, et al. Normalization of tumor vessels by lenvatinib-based metallonanodrugs alleviates hypoxia and enhances calreticulin-mediated immune responses in orthotopic HCC and organoids. Small. 2023;19: e2207786.
80. Zhang M, Wang L, Jin H, Zhao N, Liu Y, Lan S, Liu S, Zhang H. Employing single valency polyphenol to prepare metal-phenolic network antitumor reagents through FeOOH assistance. J Control Release. 2023;358:612–25.
81. Li Y. Copper homeostasis: emerging target for cancer treatment. IUBMB Life. 2020;72:1900–8.
82. Wallace KB. Nonenzymatic oxygen activation and stimulation of lipid peroxidation by doxorubicin-copper. Toxicol Appl Pharmacol. 1986;86:69–79.
83. Zheng R, Zhao L, Chen X, Liu L, Liu Y, Chen X, Wang C, Yu X, Cheng H, Li S. Metal-coordinated nanomedicine for combined tumor therapy by inducing paraptosis and apoptosis. J Control Release. 2021;336:159–68.
84. Chen M, Huang Z, Xia M, Ding Y, Shan T, Guan Z, Dai X, Xu X, Huang Y, Huang M, et al. Glutathione-responsive copper-disulfiram nanoparticles for enhanced tumor chemotherapy. J Control Release. 2022;341:351–63.
85. Ji M, Liu H, Wang H, Liang X, Wei M, Shi D, Gou J, Yin T, He H, Tang X, et al. pH-activatable copper-axitinib coordinated multifunctional nanoparticles for synergistic chemo-chemodynamic therapy against aggressive cancers. Biomater Sci. 2023;11:6267–79.
86. Huang L, Wu F, Wang Q, Meng J, Feng J, Su G, Yi X, Li Y, Li JY, Hou Z, et al. TME-triggered copper-coordinated engineered programmable

nanogenerators for on-demand cascade-amplifying oxidative stress. J Mater Chem B. 2023;11:3679–92.
87. Tang HX, Liu CG, Zhang JT, Zheng X, Yang DY, Kankala RK, Wang SB, Chen AZ. Biodegradable quantum composites for synergistic photothermal therapy and copper-enhanced chemotherapy. ACS Appl Mater Interfaces. 2020;12:47289–98.
88. Gao YM, Chiu SH, Busa P, Liu CL, Kankala RK, Lee CH. Engineered mesoporous silica-based core-shell nanoarchitectures for synergistic chemo-photodynamic therapies. Int J Mol Sci. 2022;23:11604.
89. Xiong Y, Wang Z, Wang Q, Deng Q, Chen J, Wei J, Yang X, Yang X, Li Z. Tumor-specific activatable biopolymer nanoparticles stabilized by hydroxyethyl starch prodrug for self-amplified cooperative cancer therapy. Theranostics. 2022;12:944–62.
90. Zhang G, Xie W, Xu Z, Si Y, Li Q, Qi X, Gan Y, Wu Z, Tian G. CuO dot-decorated Cu@Gd(2)O(3) core-shell hierarchical structure for Cu(i) self-supplying chemodynamic therapy in combination with MRI-guided photothermal synergistic therapy. Mater Horiz. 2021;8:1017–28.
91. Chang L, Huang H, Feng W, Fu H, Qi F, Liu J, Chen Y. Programmed self-assembly of enzyme activity-inhibited nanomedicine for augmenting chemodynamic tumor nanotherapy. Nanoscale. 2022;14:6171–83.
92. Zhang WX, Hao YN, Gao YR, Shu Y, Wang JH. Mutual benefit between Cu(II) and polydopamine for improving photothermal-chemodynamic therapy. ACS Appl Mater Interfaces. 2021;13:38127–37.
93. Liu C, Jia S, Tu L, Yang P, Wang Y, Ke S, Shi W, Ye S. GSH-responsive and hypoxia-activated multifunctional nanoparticles for synergetically enhanced tumor therapy. ACS Biomater Sci Eng. 2022;8:1942–55.
94. Sun X, Liang X, Wang Y, Ma P, Xiong W, Qian S, Cui Y, Zhang H, Chen X, Tian F, et al. A tumor microenvironment-activatable nanoplatform with phycocyanin-assisted in-situ nanoagent generation for synergistic treatment of colorectal cancer. Biomaterials. 2023;301: 122263.
95. Hossan MS, Break MKB, Bradshaw TD, Collins HM, Wiart C, Khoo TJ, Alafnan A. Novel semi-synthetic Cu (II)-cardamonin complex exerts potent anticancer activity against triple-negative breast and pancreatic cancer cells via inhibition of the akt signaling pathway. Molecules. 2021;26:2166.
96. Caro-Ramírez JY, Rivas MG, Gonzalez PJ, Williams PAM, Naso LG, Ferrer EG. Copper(II) cation and bathophenanthroline coordination enhance therapeutic effects of naringenin against lung tumor cells. Biometals. 2022;35:1059–76.
97. Emami F, Aliomrani M, Tangestaninejad S, Kazemian H, Moradi M, Rostami M. Copper-curcumin-bipyridine dicarboxylate complexes as anticancer candidates. Chem Biodivers. 2022;19: e202200202.
98. Huang Z, Ding Y, Luo Y, Chen M, Zeng Z, Zhang T, Sun Y, Huang Y, Zhao C. ROS-triggered cycle amplification effect: a prodrug activation nano-amplifier for tumor-specific therapy. Acta Biomater. 2022;152:367–79.
99. Zhu F, Huang C, Lin Y, Li Y, Tu R, Lu W. Self-delivery of a metal-coordinated anti-angiogenic nanodrug with GSH depleting ability for synergistic chemo-phototherapy. Biomater Sci. 2023;11:7132–45.
100. Chen L, Zuo W, Xiao Z, Jin Q, Liu J, Wu L, Liu N, Zhu X. A carrier-free metal-coordinated dual-photosensitizers nanotheranostic with glutathione-depletion for fluorescence/photoacoustic imaging-guided tumor phototherapy. J Colloid Interface Sci. 2021;600:243–55.
101. Kim S, Seo JH, Jeong DI, Yang M, Lee SY, Lee J, Cho HJ. Fenton-like reaction, glutathione reduction, and photothermal ablation-built-in hydrogels crosslinked by cupric sulfate for loco-regional cancer therapy. Biomater Sci. 2021;9:847–60.
102. Li X, Xi D, Yang M, Sun W, Peng X, Fan J. An organic nanotherapeutic agent self-assembled from cyanine and Cu (II) for combined photothermal and chemodynamic therapy. Adv Healthc Mater. 2021;10: e2101008.
103. Zhao L, Zheng R, Liu L, Chen X, Guan R, Yang N, Chen A, Yu X, Cheng H, Li S. Self-delivery oxidative stress amplifier for chemotherapy sensitized immunotherapy. Biomaterials. 2021;275: 120970.
104. Wang YE, Zhai J, Zheng Y, Pan J, Liu X, Ma Y, Guan S. Self-assembled iRGD-R7-LAHP-M nanoparticle induced sufficient singlet oxygen and enhanced tumor penetration immunological therapy. Nanoscale. 2022;14:11388–406.
105. Wang Y, Ding Y, Yao D, Dong H, Ji C, Wu J, Hu Y, Yuan A. Copper-based nanoscale coordination polymers augmented tumor radioimmunotherapy for immunogenic cell death induction and T-cell infiltration. Small. 2021;17: e2006231.
106. Tsvetkov P, Coy S, Petrova B, Dreishpoon M, Verma A, Abdusamad M, Rossen J, Joesch-Cohen L, Humeidi R, Spangler RD, et al. Copper induces cell death by targeting lipoylated TCA cycle proteins. Science. 2022;375:1254–61.
107. Pi W, Wu L, Lu J, Lin X, Huang X, Wang Z, Yuan Z, Qiu H, Zhang J, Lei H, et al. A metal ions-mediated natural small molecules carrier-free injectable hydrogel achieving laser-mediated photo-Fenton-like anticancer therapy by synergy apoptosis/cuproptosis/anti-inflammation. Bioact Mater. 2023;29:98–115.
108. Jia W, Tian H, Jiang J, Zhou L, Li L, Luo M, Ding N, Nice EC, Huang C, Zhang H. Brain-targeted HFn-Cu-REGO nanoplatform for site-specific delivery and manipulation of autophagy and cuproptosis in glioblastoma. Small. 2023;19: e2205354.
109. Chen J, Zhu Y, Kaskel S. Porphyrin-based metal-organic frameworks for biomedical applications. Angew Chem Int Ed Engl. 2021;60:5010–35.
110. Han D, Liu X, Wu S. Metal organic framework-based antibacterial agents and their underlying mechanisms. Chem Soc Rev. 2022;51:7138–69.
111. Horcajada P, Chalati T, Serre C, Gillet B, Sebrie C, Baati T, Eubank JF, Heurtaux D, Clayette P, Kreuz C, et al. Porous metal-organic-framework nanoscale carriers as a potential platform for drug delivery and imaging. Nat Mater. 2010;9:172–8.
112. Liu Y, Wu J, Li W, Li J, Han H, Song Z. Responsive metal–organic framework nanocarrier delivery system: an effective solution against bacterial infection. Coord Chem Rev. 2023;496: 215431.
113. Li J, Du N, Tan Y, Hsu HY, Tan C, Jiang Y. Conjugated polymer nanoparticles based on copper coordination for real-time monitoring of pH-responsive drug delivery. ACS Appl Bio Mater. 2021;4:2583–90.
114. Wang Y, Xu S, Shi L, Teh C, Qi G, Liu B. Cancer-cell-activated in situ synthesis of mitochondria-targeting AIE photosensitizer for precise photodynamic therapy. Angew Chem Int Ed Engl. 2021;60:14945–53.
115. Wu S, Hu S, Yang X. Dual drug loaded, pH-sensitive metal-organic particles for synergistic cancer therapy. Front Bioeng Biotechnol. 2022;10: 945148.
116. Tsymbal SA, Moiseeva AA, Agadzhanian NA, Efimova SS, Markova AA, Guk DA, Krasnovskaya OO, Alpatova VM, Zaitsev AV, Shibaeva AV, et al. Copper-containing nanoparticles and organic complexes: metal reduction triggers rapid cell death via oxidative burst. Int J Mol Sci. 2021;22:11065.
117. Sun P, Jia L, Hai J, Lu S, Chen F, Liang K, Sun S, Liu H, Fu X, Zhu Y, et al. Tumor microenvironment-"AND" near-infrared light-activated coordination polymer nanoprodrug for on-demand co-sensitized synergistic cancer therapy. Adv Healthc Mater. 2021;10: e2001728.
118. Yu J, Wang Y, Zhou S, Li J, Wang J, Chi D, Wang X, Lin G, He Z, Wang Y. Remote loading paclitaxel-doxorubicin prodrug into liposomes for cancer combination therapy. Acta Pharm Sin B. 2020;10:1730–40.
119. Xiong K, Zhou Y, Karges J, Du K, Shen J, Lin M, Wei F, Kou J, Chen Y, Ji L, et al. Autophagy-dependent apoptosis induced by apoferritin-Cu(II) nanoparticles in multidrug-resistant colon cancer cells. ACS Appl Mater Interfaces. 2021;13:38959–68.
120. Guo Y, Fan Y, Wang Z, Li G, Zhan M, Gong J, Majoral JP, Shi X, Shen M. Chemotherapy mediated by biomimetic polymeric nanoparticles potentiates enhanced tumor immunotherapy via amplification of endoplasmic reticulum stress and mitochondrial dysfunction. Adv Mater. 2022;34: e2206861.
121. Song E, Wu Q, Gao R, Lan X, Zhang Y, Geng H, Liu C, Xu F, Li Y, Liu C. Supramolecular catalytic nanomedicines based on coordination self-assembly of amino acids for cascade-activated and -amplified synergetic cancer therapy. J Mater Chem B. 2022;10:9838–47.
122. Zhou M, Tian B, Bu Y, Wu Z, Yu J, Wang S, Sun X, Zhu X, Zhou H. Enhanced pH-responsive chemo/chemodynamic synergistic cancer therapy based on In Situ Cu(2+) di-chelation. ACS Appl Bio Mater. 2023;6:3221–31.
123. Zhang L, Fu JM, Song LB, Cheng K, Zhang F, Tan WH, Fan JX, Zhao YD. Ultrasmall Bi/Cu coordination polymer combined with glucose oxidase for tumor enhanced chemodynamic therapy by starvation and photothermal treatment. Adv Healthc Mater. 2023;13: e2302264.
124. Zhou J, Xu D, Tian G, He Q, Zhang X, Liao J, Mei L, Chen L, Gao L, Zhao L, et al. Coordination-driven self-assembly strategy-activated Cu single-atom nanozymes for catalytic tumor-specific therapy. J Am Chem Soc. 2023;145:4279–93.

125. Zhang Y, Wang F, Shi L, Lu M, Lee KJ, Ditty MM, Xing Y, He HZ, Ren X, Zheng SY. Nanoscale coordination polymers enabling antioxidants inhibition for enhanced chemodynamic therapy. J Control Release. 2023;354:196–206.
126. Yang J, Wang XJ, Li SM, Jiang DX, Liu YX, Huang Y, Dong DD, Hu W, Liu B. An injectable PC(10)ARGD/Cu(2+)/DOX hydrogel for combined chemodynamic and chemotherapy of tumors. J Biomater Sci Polym Ed. 2023;35:190–205.
127. Liu T, Guo C, Xu S, Hu G, Wang L. A novel strategy to improve tumor targeting of hydrophilic drugs and nanoparticles for imaging guided synergetic therapy. Adv Healthc Mater. 2023;12: e2300883.
128. Kang R, Song M, Fang Z, Liu K. Nano-composite hydrogels of Cu-Apa micelles for anti-vasculogenic mimicry. J Drug Target. 2023;31:166–78.
129. Hu X, Song X, Yuan Y, Yao X, Chen X, Li G, Li S. Designed synthesis of prussian blue@Cu-doped zinc phosphate nanocomposites for chemo/chemodynamic/photothermal combined cancer therapy. J Mater Chem B. 2023;11:6404–11.
130. Hong Z, Zhong J, Ding D, Gong S, Zhang L, Zhao S, Shen XC, Liang H, Huang FP. A Cu(I)-based Fenton-like agent inducing mitochondrial damage for photo-assisted enhanced chemodynamic therapy. Dalton Trans. 2023;52:6187–93.
131. Lv M, Chen M, Zhang R, Zhang W, Wang C, Zhang Y, Wei X, Guan Y, Liu J, Feng K, et al. Manganese is critical for antitumor immune responses via cGAS-STING and improves the efficacy of clinical immunotherapy. Cell Res. 2020;30:966–79.
132. Zhang K, Qi C, Cai K. Manganese-based tumor immunotherapy. Adv Mater. 2023;35: e2205409.
133. Jiang W, Wang Q, Cui D, Han L, Chen L, Xu J, Niu N. Metal-polyphenol network coated magnetic hydroxyapatite for pH-activated MR imaging and drug delivery. Colloids Surf B Biointerfaces. 2023;222: 113076.
134. Sun T, Li J, Zeng C, Luo C, Luo X, Li H. Banoxantrone coordinated metal-organic framework for photoacoustic imaging-guided high intensity focused ultrasound therapy. Adv Healthc Mater. 2023;12: e2202348.
135. Lv X, Huang J, Min J, Wang H, Xu Y, Zhang Z, Zhou X, Wang J, Liu Z, Zhao H. Multi-signaling pathway activation by pH responsive manganese particles for enhanced vaccination. J Control Release. 2023;357:109–19.
136. Geng Z, Chen F, Wang X, Wang L, Pang Y, Liu J. Combining anti-PD-1 antibodies with Mn(2+)-drug coordinated multifunctional nanoparticles for enhanced cancer therapy. Biomaterials. 2021;275: 120897.
137. Liu K, Zhang L, Lu H, Wen Y, Bi B, Wang G, Jiang Y, Zeng L, Zhao J. Enhanced mild-temperature photothermal therapy by pyroptosis-boosted ATP deprivation with biodegradable nanoformulation. J Nanobiotechnology. 2023;21:64.
138. Sun X, Zhang Y, Li J, Park KS, Han K, Zhou X, Xu Y, Nam J, Xu J, Shi X, et al. Amplifying STING activation by cyclic dinucleotide-manganese particles for local and systemic cancer metalloimmunotherapy. Nat Nanotechnol. 2021;16:1260–70.
139. Yan J, Wang G, Xie L, Tian H, Li J, Li B, Sang W, Li W, Zhang Z, Dai Y. Engineering radiosensitizer-based metal-phenolic networks potentiate STING pathway activation for advanced radiotherapy. Adv Mater. 2022;34: e2105783.
140. Dai Y, Li X, Xue Y, Chen K, Jiao G, Zhu L, Li M, Fan Q, Dai Y, Zhao Q, et al. Self-delivery of metal-coordinated NIR-II nanoadjuvants for multimodal imaging-guided photothermal-chemodynamic amplified immunotherapy. Acta Biomater. 2023;166:496–511.
141. Liu P, Liu X, Cheng Y, Zhong S, Shi X, Wang S, Liu M, Ding J, Zhou W. Core-shell nanosystems for self-activated drug-gene combinations against triple-negative breast cancer. ACS Appl Mater Interfaces. 2020;12:53654–64.
142. Nie Y, Li D, Peng Y, Wang S, Hu S, Liu M, Ding J, Zhou W. Metal organic framework coated MnO(2) nanosheets delivering doxorubicin and self-activated DNAzyme for chemo-gene combinatorial treatment of cancer. Int J Pharm. 2020;585: 119513.
143. Wu Y, Xu L, Qian J, Shi L, Su Y, Wang Y, Li D, Zhu X. Methotrexate-Mn(2+) based nanoscale coordination polymers as a theranostic nanoplatform for MRI guided chemotherapy. Biomater Sci. 2020;8:712–9.
144. Geng P, Yu N, Liu X, Wen M, Ren Q, Qiu P, Macharia DK, Zhang H, Li M, Chen Z. GSH-sensitive nanoscale Mn(3+)-sealed coordination particles as activatable drug delivery systems for synergistic photodynamic-chemo therapy. ACS Appl Mater Interfaces. 2021;13:31440–51.
145. Chen X, Fan X, Zhang Y, Wei Y, Zheng H, Bao D, Xu H, Piao JG, Li F, Zheng H. Cooperative coordination-mediated multi-component self-assembly of "all-in-one" nanospike theranostic nano-platform for MRI-guided synergistic therapy against breast cancer. Acta Pharm Sin B. 2022;12:3710–25.
146. Zhang M, Jia C, Zhuang J, Hou YY, He XW, Li WY, Bai G, Zhang YK. GSH-responsive drug delivery system for active therapy and reducing the side effects of bleomycin. ACS Appl Mater Interfaces. 2022;14:417–27.
147. Cao H, Jiang B, Yang Y, Zhao M, Sun N, Xia J, Gao X, Li J. Cell membrane covered polydopamine nanoparticles with two-photon absorption for precise photothermal therapy of cancer. J Colloid Interface Sci. 2021;604:596–603.
148. Lin L, Yu J, Lu H, Wei Z, Chao Z, Wang Z, Wu W, Jiang H, Tian L. Mn-DNA coordination of nanoparticles for efficient chemodynamic therapy. Chem Commun. 2021;57:1734–7.
149. Jomova K, Makova M, Alomar SY, Alwasel SH, Nepovimova E, Kuca K, Rhodes CJ, Valko M. Essential metals in health and disease. Chem Biol Interact. 2022;367: 110173.
150. Lei L, Dong Z, Xu L, Yang F, Yin B, Wang Y, Yue R, Guan G, Xu J, Song G, et al. Metal-fluorouracil networks with disruption of mitochondrion enhanced ferroptosis for synergistic immune activation. Theranostics. 2022;12:6207–22.
151. Zou Z, He L, Deng X, Wang H, Huang Z, Xue Q, Qing Z, Lei Y, Yang R, Liu J. Zn(2+) -coordination-driven RNA assembly with retained integrity and biological functions. Angew Chem Int Ed Engl. 2021;60:22970–6.
152. Jiang Z, Wang T, Yuan S, Wang M, Qi W, Su R, He Z. A tumor-sensitive biological metal-organic complex for drug delivery and cancer therapy. J Mater Chem B. 2020;8:7189–96.
153. Gao H, Chu C, Cheng Y, Zhang Y, Pang X, Li D, Wang X, Ren E, Xie F, Bai Y, et al. In Situ formation of nanotheranostics to overcome the blood-brain barrier and enhance treatment of orthotopic glioma. ACS Appl Mater Interfaces. 2020;12:26880–92.
154. Jiang Z, Li T, Cheng H, Zhang F, Yang X, Wang S, Zhou J, Ding Y. Nano-medicine potentiates mild photothermal therapy for tumor ablation. Asian J Pharm Sci. 2021;16:738–61.
155. Wang JL, Hu XY, Han CG, Hou SY, Wang HS, Zheng F. Lanthanide complexes for tumor diagnosis and therapy by targeting sialic acid. ACS Nano. 2022;16:14827–37.
156. Hu H, Yang N, Sun J, Zhou F, Gu R, Liu Y, Wang L, Song X, Yun R, Dong X, et al. Zn(ii)-Coordination-driven self-assembled nanoagents for multimodal imaging-guided photothermal/gene synergistic therapy. Chem Sci. 2022;13:7355–64.
157. Lei J, Zhang W, Ma L, He Y, Liang H, Zhang X, Li G, Feng X, Tan L, Yang C. Sonodynamic amplification of cGAS-STING activation by cobalt-based nanoagonist against bone and metastatic tumor. Biomaterials. 2023;302: 122295.
158. Zhen W, Liu Y, An S, Jiang X. Glutathione-induced In Situ Michael Addition between nanoparticles for pyroptosis and immunotherapy. Angew Chem Int Ed Engl. 2023;62: e202301866.
159. Yang S, Li D, Chen L, Zhou X, Fu L, You Y, You Z, Kang L, Li M, He C. Coupling metal organic frameworks with molybdenum disulfide nanoflakes for targeted cancer theranostics. Biomater Sci. 2021;9:3306–18.
160. Pellerito C, Emanuele S, Ferrante F, Celesia A, Giuliano M, Fiore T. Tributyltin(IV) ferulate, a novel synthetic ferulic acid derivative, induces autophagic cell death in colon cancer cells: From chemical synthesis to biochemical effects. J Inorg Biochem. 2020;205: 110999.
161. Tikhonov S, Ostroverkhov P, Suvorov N, Mironov A, Efimova Y, Plutinskaya A, Pankratov A, Ignatova A, Feofanov A, Diachkova E, et al. Tin carboxylate complexes of natural bacteriochlorin for combined photodynamic and chemotherapy of cancer è. Int J Mol Sci. 2021;22:13563.
162. Hosseini-Kharat M, Rahimi R, Alizadeh AM, Zargarian D, Khalighfard S, Mangin LP, Mahigir N, Ayati SH, Momtazi-Borojeni AA. Cytotoxicity, anti-tumor effects and structure-activity relationships of nickel and palladium S, C, S pincer complexes against double and triple-positive and triple-negative breast cancer (TNBC) cel*ls*. Bioorg Med Chem Lett. 2021;43: 128107.
163. Amaral L, Moniz T, Silva AMN, Rangel M. Vanadium compounds with antidiabetic potential. Int J Mol Sci. 2023;24:15675.
164. Ścibior A, Pietrzyk Ł, Plewa Z, Skiba A. Vanadium: Risks and possible benefits in the light of a comprehensive overview of its

pharmacotoxicological mechanisms and multi-applications with a summary of further research trends. J Trace Elem Med Biol. 2020;61: 126508.
165. Treviño S, Diaz A. Vanadium and insulin: partners in metabolic regulation. J Inorg Biochem. 2020;208: 111094.
166. Li S, Chen Y, Zhu W, Yang W, Chen Z, Song J, Song X, Chen X, Yang H. engineered nanoscale vanadium metallodrugs for robust tumor-specific imaging and therapy. Adv Func Mater. 2021;31:2010337.
167. Chen T, Huang R, Liang J, Zhou B, Guo XL, Shen XC, Jiang BP. Natural polyphenol-vanadium oxide nanozymes for synergistic chemodynamic/photothermal therapy. Chemistry. 2020;26:15159–69.
168. Hu D, Xu H, Zhang W, Xu X, Xiao B, Shi X, Zhou Z, Slater NKH, Shen Y, Tang J. Vanadyl nanocomplexes enhance photothermia-induced cancer immunotherapy to inhibit tumor metastasis and recurrence. Biomaterials. 2021;277: 121130.
169. Liu P, Shi X, Peng Y, Hu J, Ding J, Zhou W. Anti-PD-L1 DNAzyme loaded photothermal Mn(2+) /Fe(3+) hybrid metal-phenolic networks for cyclically amplified tumor ferroptosis-immunotherapy. Adv Healthc Mater. 2022;11: e2102315.
170. Wang D, Zhang N, Yang T, Zhang Y, Jing X, Zhou Y, Long J, Meng L. Amino acids and doxorubicin as building blocks for metal ion-driven self-assembly of biodegradable polyprodrugs for tumor theranostics. Acta Biomater. 2022;147:245–57.
171. Singh S, Pal K. Folic-acid adorned alginate-polydopamine modified paclitaxel/Zn-CuO nanocomplex for pH triggered drug release and synergistic antitumor efficacy. Int J Biol Macromol. 2023;234: 123602.
172. Malagrino TRS, Godoy AP, Barbosa JM, Lima AGT, Sousa NCO, Pedrotti JJ, Garcia PS, Paniago RM, Andrade LM, Domingues SH, et al. Multifunctional hybrid MoS(2)-pegylated/Au nanostructures with potential theranostic applications in biomedicine. Nanomaterials. 2022;12:2053.
173. Pham SQT, Assadawi N, Wells J, Sophocleous RA, Davis KJ, Yu H, Sluyter R, Dillon CT, Kelso C, Beck JL, et al. A new class of quadruplex DNA-binding nickel Schiff base complexes. Dalton Trans. 2020;49:4843–60.
174. Argitekin E, Ersoz-Gulseven E, Cakan-Akdogan G, Akdogan Y. Dopamine-conjugated bovine serum albumin nanoparticles containing pH-responsive catechol-V(III) coordination for In Vitro and In Vivo drug delivery. Biomacromol. 2023;24:3603–18.
175. Zhang Y, Du X, He Z, Gao S, Ye L, Ji J, Yang X, Zhai G. A vanadium-based nanoplatform synergizing ferroptotic-like therapy with glucose metabolism intervention for enhanced cancer cell death and antitumor immunity. ACS Nano. 2023;17:11537–56.
176. Xu M, Zha H, Han R, Cheng Y, Chen J, Yue L, Wang R, Zheng Y. Cyclodextrin-derived ROS-generating nanomedicine with pH-modulated degradability to enhance tumor ferroptosis therapy and chemotherapy. Small. 2022;18: e2200330.
177. Kontoghiorghes GJ. Iron load toxicity in medicine: from molecular and cellular aspects to clinical implications. Int J Mol Sci. 2023;24:12928.
178. Stiles LI, Ferrao K, Mehta KJ. Role of zinc in health and disease. Clin Exp Med. 2024;24:38.
179. Berger MM, Shenkin A, Dizdar OS, Amrein K, Augsburger M, Biesalski HK, Bischoff SC, Casaer MP, Gundogan K, Lepp HL, et al. ESPEN practical short micronutrient guideline. Clin Nutr. 2024;43:825–57.
180. Najahi-Missaoui W, Arnold RD, Cummings BS. Safe nanoparticles: are we there yet? Int J Mol Sci. 2020;22:385.

Publisher's Note